COMMUNICATIONS IN STATISTICS: CASE STUDIES, DATA ANALYSIS AND APPLICATIONS
https://doi.org/10.1080/23737484.2026.2630287

Development of data-driven statistical models for daily water table depth prediction and variable selection: Two case studies in coastal plain forested wetlands

Alokesh Manna[a], Sushant Mehan[b], and Devendra M. Amatya[c]

[a]Department of Statistics, University of Connecticut, Storrs, CT, USA; [b]Department of Agricultural and Biosystems Engineering, South Dakota State University, Brookings, SD, USA; [c]USDA Forest Service Santee Experimental Forest, Center for Forest Watershed Research, Cordesville, SC, USA

ABSTRACT

Accurately predicting water table dynamics is vital for sustaining groundwater resources, ecological functions, and anthropogenic activities. This study evaluates autoregressive model with a) prediction under sparsity assumption within model coefficients, b) allows lags present in both dependent and independent variables for estimating daily water table depth using hydroclimatic data from the USDA Forest Service Santee Experimental Forest (SC) and D1 (NC). Data from 2006–2019 (SC) and 1988–2008 (NC) were used, with predictors including soil and air temperature, precipitation, wind, and radiation. For WS80, RMSE during the dormant season was 10.09cm, with daily testing phase RMSE 14.94cm. The model achieved an R^2 0.93 for 2019 (dry year) and 0.96 for 2016 (wet year). Solar radiation, rainfall, and wind direction were among the most influential variables. This predictive model can aid forest managers and hydrologists in using water tables for assessing wetland hydrology and related ecosystem functions in management decisions and provide out-of-sample prediction with reasonable accuracy.

ARTICLE HISTORY
Received 17 August 2025
Accepted 4 February 2026

KEYWORDS
Autoregressive; Hydrology; time series modeling; variable selection; water table depth

1. Introduction

Water table depth plays a crucial role in silviculture management, influencing various ecological and hydrological processes essential for forest health and productivity. Understanding water table dynamics is vital for effective forest management practices, as it directly affects tree growth, species composition, and overall forest ecosystem resilience. Firstly, water table depth significantly impacts vegetation growth and health. Optimal water table levels are critical for sustaining plant biomass and root development. For instance, studies indicate

CONTACT Alokesh Manna alokesh.manna@uconn.edu Department of Statistics, University of Connecticut, Storrs, CT 06269, USA.

Supplemental data for this article can be accessed on the publisher's website.

that a water table depth of approximately 3 meters is ideal for preventing land desertification and promoting healthy vegetation growth, as it maintains a suitable water balance and mitigates soil salinization (Cui and Shao 2005). Additionally, research has shown that variations in water table depth can lead to substantial differences in root growth and biomass accumulation in species such as *Populus alba*, highlighting the importance of maintaining appropriate water levels for silvicultural success (Imada, Yamanaka, and Tamai 2008).

Moreover, the relationship between water table depth and forest management practices is evident in hydrology and nutrient cycling. Silvicultural activities, such as harvesting and thinning, can alter water table levels and affect hydrological processes. For example, studies have demonstrated significant changes in hydrology and nutrient concentrations on forest sites due to silvicultural operations, including a decrease in water table levels immediately following forest harvesting, which can impact water quantity and quality (Ssegane et al. 2017; Appelboom et al. 2006). Effective management practices that consider water table dynamics can help mitigate these impacts, ensuring that forest ecosystems remain resilient to disturbances such as drought and pest infestations (Pinno et al. 2021; Del Campo, Fernandes, and Molina 2014).

Furthermore, integrating water-oriented silvicultural practices is becoming increasingly important in adaptive forest management strategies, particularly in semiarid regions. These practices aim to balance the ecological needs of forests with human water use, thereby enhancing the sustainability of forest ecosystems (Del Campo, Fernandes, and Molina 2014; Manrique-Alba, del Campo, and Gonzalez-Sanchis 2015). By understanding the hydrological implications of silvicultural practices, forest managers can implement strategies that optimize water use while maintaining forest health and productivity.

This is why estimating water table depth in forested ecosystems is essential for understanding hydrological dynamics and managing forest resources effectively. Various simulation methods have been developed to model water table depth, each with unique approaches and applications. This synthesis discusses several prominent simulation methods, highlighting their strengths and limitations. One of the widely used models for simulating daily water table depth is the DRAINMOD (Tian et al. 2012; Grace III, Skaggs, and Chescheir 2006; Amatya et al. 2024). Dai et al. (2010) describes another useful model MIKE SHE (originally developed by Graham and Butts 2005) which incorporates streamflow and water table depth to describe a hydrological process for a forested SC coastal plane. Sun, Riekerk, and Comerford (1998) developed a model FLATWOOD for the forest hydrology of the wetland-upland ecosystem in Florida with daily precipitation and temperature.

The integration of hydrological models with remote sensing techniques has also gained traction in estimating water table depth. For example, studies have demonstrated that satellite-derived data, such as the Normalized Difference Vegetation Index (NDVI), can be effectively used to assess water conservation and its relationship with water table levels in different ecosystems, including forests (Zhang et al. 2021). Zhang et al. (2021) provides a spatially explicit approach to monitor water table changes over large areas, although the inherent variability of vegetation cover and other environmental factors may influence it.

Furthermore, machine learning algorithms have emerged as a promising method for estimating water table depth. These algorithms can analyze vast datasets to identify patterns and relationships between various environmental variables and water table levels. For instance, explored the inherent water-use efficiency of different forest ecosystems, demonstrating how machine learning can enhance the understanding of water dynamics about climatic variables (Liu et al. 2022). This approach allows for more accurate predictions of water table depth, particularly in the context of changing climate conditions. Lastly, the application of hydrological models that account for evapotranspiration processes is critical for estimating water table depth. Models that incorporate spatial evapotranspiration estimation methods have shown that inaccuracies in estimating this process can lead to significant uncertainties in hydrological simulations (Xuan et al. 2016). One of the most prominent algorithms used for estimating water table depth is the Random Forest (RF) algorithm. This ensemble learning method has been shown to effectively model the depth to shallow groundwater at high spatial resolutions. For instance, demonstrated the applicability of RF in producing detailed maps that capture extreme conditions, such as wintertime water table depths, highlighting its robustness in handling non-linear relationships and interactions among predictors (Koch et al. 2019).

The RF algorithm's ability to manage large datasets and its resistance to overfitting make it particularly suitable for hydrological modeling in diverse forest environments. Support Vector Machines (SVM) have also been utilized to estimate water table depth. This method effectively classifies and regresses data, making it a valuable tool for predicting water table levels based on various input features. Additionally, machine learning techniques such as Artificial Neural Networks (ANNs) and Gradient Boosting (GB) have been applied in similar contexts. For example, explored various machine learning methods, including ANN and GB, for predicting water table depth in seasonal freezing-thawing areas. Their findings indicated that these methods could effectively capture the temporal fluctuations of water tables influenced by climatic and land-use changes (Zhao et al. 2020). The adaptability of these algorithms to different environmental conditions enhances their applicability in forest ecosystems.

Moreover, the integration of multiple machine learning algorithms has been proposed to improve prediction accuracy. For instance, the combination of RF and other models can leverage the strengths of each method, resulting in more reliable estimates of water table depth.

In this study, we will investigate the performance of a statistical model with optimization techniques to predict daily and seasonal (growing season (April 1–Oct 30) and dormant season (November 1–March 31)) water table depth

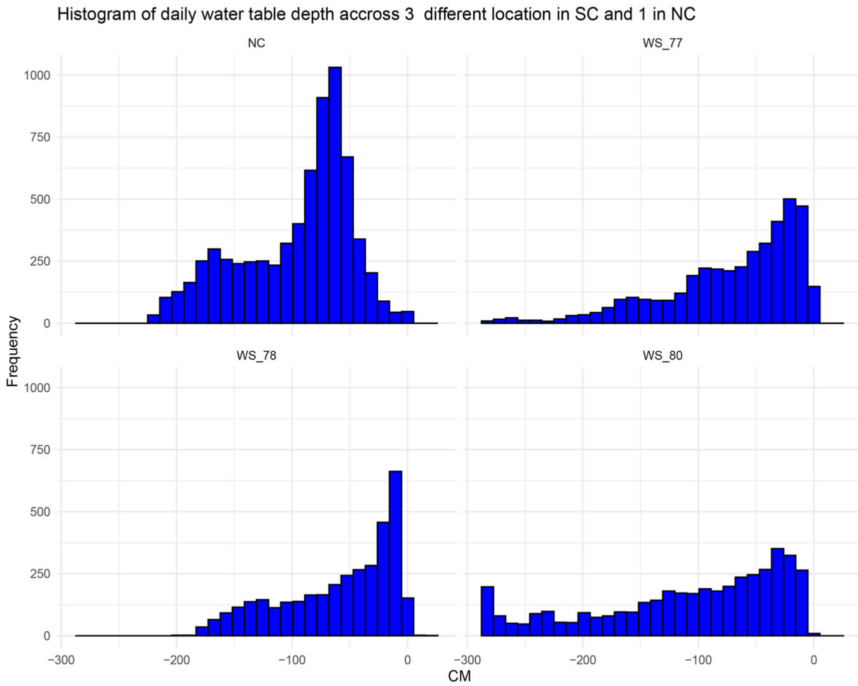

(a)

Figure 1. Histogram of daily water table depth (cm) across three different well locations in watersheds WS77 and WS78 in SC and one in watershed D1 in NC.

and elevation using available meteorological and hydrological data. Weather and ecohydrology data, recorded at the USDA Forest Service Experimental Forest sites in South Carolina, have been used to predict water table dynamics. Initially, we explored data from three hydro-meteorological stations across three watersheds: WS77, WS78, and WS80 (see Figs. 1 and 2). In Fig. 1, D1 (NC) has a relatively consistent and narrow distribution around −50 cm, indicating a stable water table depth around that range.

WS77 shows a much narrower range and predominantly shallow water table depths, close to 0 cm. WS78 has a broader distribution with more variance in water table depths, extending to much deeper levels than WS77. WS80 shows multiple peaks, suggesting variability, with many occurrences at deeper water table depths, more so than at the other locations. In Fig. 2 we can observe that for the dormant period, the water table depths during the dormant period are relatively shallow, with most values concentrated near 0 cm or slightly deeper for WS77 and WS78. However, the histogram shows a slight shift towards relatively deeper depths during the dormant period, with frequent water table depths around −100 cm or shallower but stays so for a longer period than WS77 and WS78 for WS80 in the dormant season. For the growing period, the water table depths are much deeper, with frequent values between −100 cm and −200

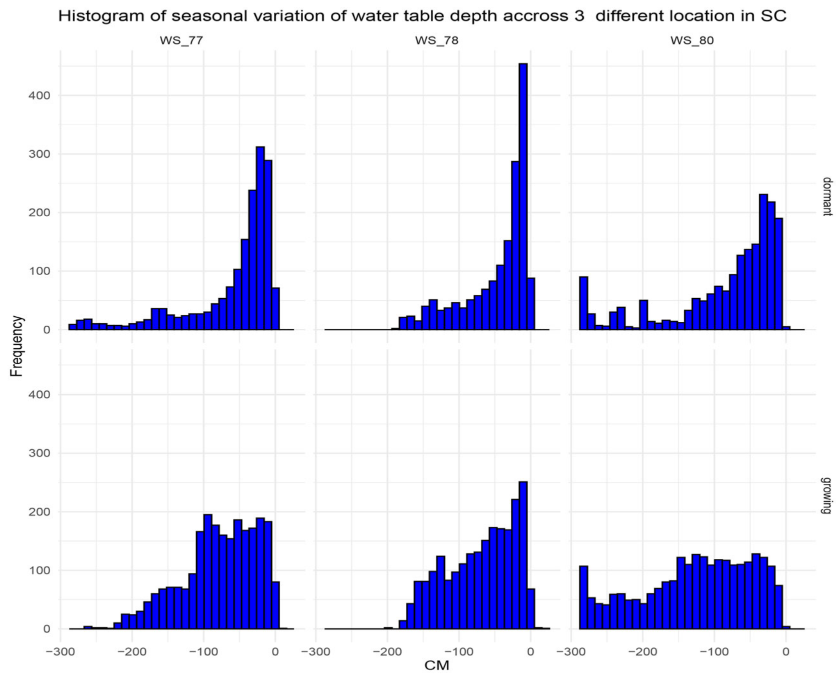

(a)

Figure 2. Histogram of daily water table depths (cm) for wells on watersheds WS77, WS78 and WS80 in SC for growing and dormant.

cm for WS77, WS78, and WS80 as expected due to higher evapotranspiration demand. The water table distribution is more spread out, indicating greater variability in water table depths during this period.

Water table depth in the soil is one important hydrologic variable that affects the growth of trees and biodiversity on the earth's surface. The water table, as used routinely by hydrologists in various disciplines, is seemingly a simple concept, that marks the top of the saturated zone in porous media (see Baird and Low (2022)). The position of the water table relative to the ground surface—that is, water-table depth (WTD)—has also proved useful as an indicator of soil aeration and biochemical conditions of the soil. In addition, water table is also used to quantify and understand groundwater resources (Baird and Low (2022)). The authors also cited references indicating relationships between water table depth and many other variables, including soil greenhouse gas emissions, plant rooting depth, primary productivity, crop yield, and the species composition of wetland vegetation.

Similarly, Vepraskas, Skaggs, and Caldwell (2020) used the water table depth to examine wetland hydrology on forested lands. These relationships exist because the water table is a proxy for the degree of waterlogging, soil redox status, and water availability. Therefore, an accurate prediction of water table dynamics is important. Amatya and Skaggs (2001) discussed the water table depth prediction in pine plantations of poorly drained soils. It was concluded that the model is a reliable tool for assessing the hydrologic impacts of silvicultural and water management treatments, as well as climate changes on these pine stands. Tian et al. (2012) has discussed the hydrology behavior in the presence of different chemical components in the soil and the effect on plant growth in drained soil. This application of DRAINMOD-FOREST demonstrated its capability for predicting hydrology and Carbon and Nitrogen dynamics in drained forests under limited silvicultural practices. Amatya, Fialkowski, and Bitner (2019) discussed a methodology for water table depth prediction based on a differential equation with several available weather covariates such as rainfall, PET (potential evapotranspiration), etc.

Recent studies have increasingly explored data-driven and machine learning approaches for water table forecasting, complementing traditional statistical and hydrological models. Wunsch, Liesch, and Broda (2020) compared LSTM, convolutional neural networks (CNNs), and NARX models for groundwater level prediction, highlighting that while deep learning models can capture complex dynamics, simpler NARX models often perform competitively in data-limited settings. Zhang et al. (2023) applied temporal convolutional networks (TCNs) and LSTMs to forecast coastal groundwater levels, demonstrating improved predictive accuracy over classical approaches across varying lead times. Janssen, Tootchi, and Ameli (2024) critically evaluated machine learning models for regional water table estimation, emphasizing challenges in interpretability and uncertainty quantification despite strong predictive performance. More recently, Salis et al. (2025) developed time-distributed deep learning architectures that transform weather image sequences into daily water table predictions, illustrating the potential of exogenous, purely data-driven frameworks. Together, these studies reflect a clear trend toward hybrid and fully data-driven modeling in groundwater hydrology, situating our BigVAR-based, interpretable approach within a contemporary context of predictive water table modeling.

The proposed model predicts water table depth for poorly drained high water table soils, with the potential for assessing the effects of land management, wetland hydrology, and climate changes. Existing literature has addressed the water table depth estimation through the machine learning procedure. Zhao et al. (2020) approached water table dynamics estimation with support vector regression. It was concluded that a water table depth of less than 3.64 billion m3 of water diversion might result in risks of environmental problems. Herath et al. (2023) addressed the water level prediction model for the Colombo flood detention area using a feed-forward neural network and long short-term neural network. The LSTM has outperformed FFNN and confirmed that the temporal relationship is much more robust in predicting wetland water levels than the traditional relationship. Nguyen and Phan (2020) addressed the Red River water level forecasting problem with statistical and machine learning techniques.

Autoregressive models (Hamilton 1989; Hamilton and Susmel 1994; Manna and Ghosh 2025; Manna, Mehan, and Amatya 2024) offer clear interpretability and explicit temporal dependence structures, allowing hydrologists to understand how past water table dynamics propagate into future states. Unlike many machine learning models, their parsimonious formulation reduces overfitting and ensures stable predictions even with limited environmental data.

In this study, the time series data is considered in two parts. The linear part of the time series is handled by the autoregressive integrated moving average model (ARIMA) model, and different machine learning models, such as a random forest, handle the nonlinear part. Zhu et al. (2020) have a review paper for lake water level forecasting using seven different machine learning models ANN(Artificial Neural Network), SVM (Support Vector Machine), ANFIS (Adaptive Neuro Fuzzy Inference System), hybrid models, evolutionary machine learning models, ELM (Extreme Learning Machine), and DL (Deep Learning). This paper presents a review of the applications of ML models for modeling water-level dynamics in lakes.

Ahmed et al. (2022) discussed the problem of water level prediction using rainfall as a covariate with different methodologies such as linear regression, support vector regression, ensemble regression, XGboost, tree regression, and Gaussian process regression with a case study of the Durian Tunggal river, Malaysia. Most machine learning algorithms try to fit the nonlinearity part but lose interpretability when the data diverges from linearity or many layers in neural network models. In water table dynamics, the value at a given time point is correlated with its previous values. Lag structures help capture these autocorrelations, stationarity, and causal effects, allowing for better modeling and forecasting.

If the data is very high-dimensional with a small number of sample time points, Dawn et al. (2021, 2025) can be used for modeling change points, referring to moments in time when the statistical properties of hydrological data, such as river flow, precipitation, or groundwater levels, change abruptly. These changes might be due to natural events (like floods and droughts), climate change, human activities (like land use changes, dam construction), or other environmental factors. The available hydro-climatic variables are not also limited to affecting the water table depth at the same time point available but these variables observed several days before might have also influenced the current observed water table value. To address this problem, we have attempted to implement an auto-regressive model that incorporates lag structure on both the predictors and dependent variables, and to assess the importance of the exogenous variables or predictors in the model. We have discussed the methodology below in Sec. 4.

While these machine learning approaches achieve high predictive skill, they generally lack interpretability, making it difficult to identify the contribution of individual covariates. In contrast, our BigVAR-based model provides both accurate forecasts and interpretable coefficients, enabling explicit assessment of the influence of hydroclimatic predictors on water table dynamics. Together, these studies situate our work within a contemporary context of predictive water table modeling while highlighting the practical advantage of interpretable statistical approaches.

In our investigation, we sought to advance knowledge in modeling water table dynamics, which is critical in wetland hydrology assessment in silvicultural management. We attempted to accomplish that by selecting important variables for our inference among all available daily hydro-climatic variables for interpretability. We arranged our manuscript in the following way: in Section 1 we discussed a few available research articles for predicting water table dynamics. Section 2 described the research objective. After that, we discussed our data processing steps, implemented the model, and a few exploratory data analyses in Sec. 4. Next, we discussed our residual analysis in Sec. 7 and important variables in Sec. 7.2. Next, a discussion Sec. 8 was provided on the justification of the consideration of this model from our end and collusive remarks. We presented the recommendations and future directions of our research in Sec. 9. Lastly, we do include an acknowledgement in acknowledgement section.

2. Research objective

The key objectives of this research are the following:

- Identifying a statistical predictive model for evaluating water table depth measured at groundwater wells on three experimental watersheds WS77 , WS78, WS80 and one watershed D1 in NC across daily, monthly, growing, and dormant season temporal scales using daily hydrometeorological variables measured at the rain gauge, weather stations, and streamflow gauging stations within and/or in the vicinity of these groundwater wells as described below in Methods section.
- Statistical inference for variable selection across different temporal scales and inference.
- Daily streamflow might not commonly available in different watersheds. So we investigate how the prediction changes when daily streamflow is not incorporated when we predict water table depth.

3. Main contributions

Our model combines an autoregressive framework with a large set of hydroclimatic predictors and automatic variable selection to generate daily water table forecasts for individual watersheds, capturing temporal dependencies while identifying the most influential drivers. The key points are the following:

- We developed a novel model for predicting water table depth that incorporates sparse autoregressive coefficients. Sparse autoregressive coefficients refer to the model parameters in the autoregressive structure that are estimated to be exactly zero or close to zero using regularization techniques such as Lasso, ridge, or elastic net. This sparsity helps identify only the most influential predictors, improves model interpretability, and reduces overfitting, making the model more robust for forecasting.

- Through this approach, we identified solar radiation, rainfall, and wind direction as the key predictors of water table depth.
- The model demonstrated excellent fitting and out-of-sample predictive accuracy, showcasing its effectiveness.
- Additionally, we found that the model remained robust and performed well even when the Dailyflow variable was excluded.

4. Methods

In this section, we describe the sites from where we had collected the data, data collection with pre-processing and finally the model we are using for prediction.

4.1. Site description

The three study sites WS77, WS78, and WS80 are located at the US Forest Service Santee Experimental Forest/Center for Forested Wetlands in wetland online available dataset (https://www.fs.usda.gov/rds/archive/Catalog/RDS-2019-0033). The location diagram is given in Fig. 3. For the user, one should go to this link, and in the "Catalog/Data access:" the zip folder of the data is available. The 155-ha headwater watershed WS77 was established in 1963 as a treatment in a paired system with WS80 (control) to study the hydrologic and water quality effects of prescribed burning on poorly drained coastal plain soils. A first-order stream drains WS77 into Fox Gulley Creek, eventually flowing into Turkey Creek and then Cooper River, which leads to the Atlantic Ocean. A few pictures from the site locations are provided in Fig. 4.

Soils in WS77 belong mainly to the Wahee-Craven soil association, characterized by relatively poorly to moderately drained sandy loam to clayey soils with seasonally high water tables. The land is predominantly forested with loblolly pine, longleaf pine, and some bottomland hardwoods along the stream riparian bank. The watershed has low-gradient terrain with surface elevations ranging from 10.5 m to 5.6 m above mean sea level, with a topographic relief of up to 2% slope. The region's climate is warm-temperate, with an average daily temperature of 16°C and annual rainfall of 1375 mm, 40% of which occurs during June-August. A gauging station with a compound concrete V-notch weir at the WS77 outlet measures stream outflows. For more details please check Amoah, Amatya, and Nnaji (2013).

WS80 on the Santee Experimental Forest (SEF) was considered due to its diverse upland and wetland areas and long-term monitoring history. The 160-ha

(a) TC met station

(b) WS78 rain gauge

(c) WS80 tower station

(d) SHQ station

(e) Met 25 station

(f) Met 5 station

(g) Flow measurement station

(h) Recording logger in a gauge house

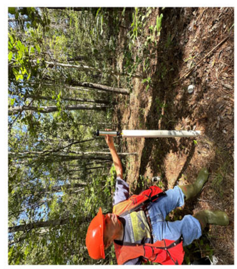

(i) Groundwater well

Figure 3. Photos of various hydro-meteorologic measuring equipment on the study watersheds. Met 5 and Met 25 are satellite stations measuring air temperature, soil temperature, and precipitation on WS77 and WS80, respectively. TC met is the complete weather station on the WS78 watershed. SHQ is another full-weather station in the headquarters office.

watershed WS80 serves as the control watershed for a paired system with WS77 within the larger second-order watershed WS79 (500 ha), which drains into Huger Creek, a tributary of the East Branch draining to the Cooper River. A gauging station with a compound concrete V-notch weir at the WS80 outlet measures stream outflows dating back to 1968.

The watershed's topography is planar with a slope of less than 4%, and the elevation ranges from 4 to 10 m above mean sea level. Soils in WS80, developed from coastal plain sediments, are hydric and moderately well-drained in upland areas but poorly drained in the riparian zone. The main soil type is loamy, covering about 90% of the watershed. Topsoil clay content is 30% while subsoil clay content is 40–60%The forest vegetation on WS80 has remained unregulated

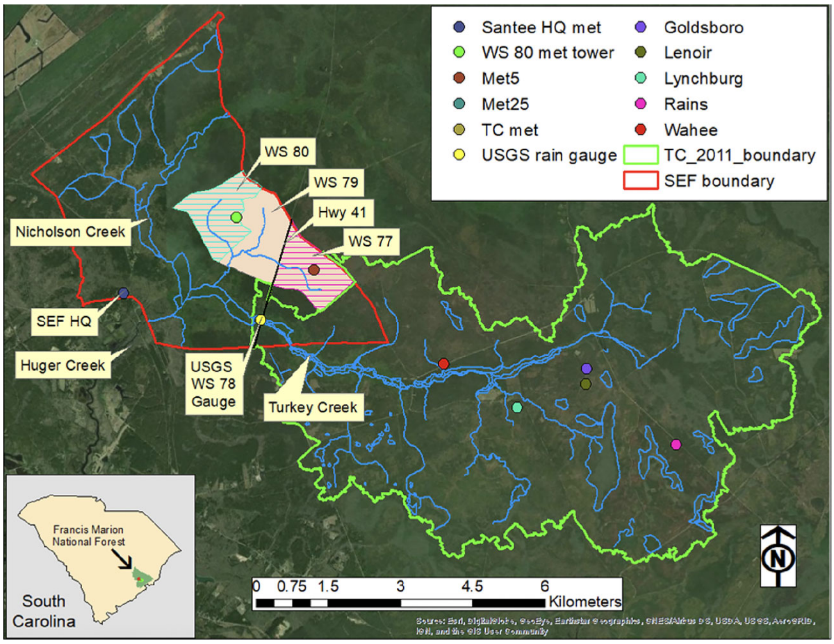

Figure 4. Location map of study watersheds WS77 and WS80 with Met5 and Met25, satellite stations, respectively, WS78 (Turkey Creek) in green boundary with TC met, a complete SEF HQ weather station, and the SEF HQ, another full-weather station at the Santee headquarters office (Mehan, Manna, and Amatya 2025).

for over five decades, despite being heavily impacted by Hurricane Hugo in 1989. The site was left to regenerate naturally without biomass removal or salvage logging. A detailed description of this study site is available in Dai et al. (2010).

The third study site is the Turkey Creek watershed (WS78) in the Santee Experimental Forest. The WS78 gauging station was instrumented with a real-time stream gauge sensor and a rain gauge (rain gauge, accessed on 20 February 2024) since 2005 and is managed in cooperation with the US Geological Survey (USGS) and the College of Charleston, but its monitoring has just been discontinued.

This watershed is a headwater of the East Branch of the Cooper River, which drains into Charleston Harbor. The Turkey Creek watershed, similar to other low-gradient forest watersheds in the southeastern Atlantic coastal plain, has experienced rapid urban development since the 1990s. The elevation ranges from 3.5 m at the outlet to 11.5 m above mean sea level.

The watershed's land use comprises 88% pine forest (mainly regenerated loblolly and longleaf pine), 10% wetlands and water, and 2% agricultural lands, roads, and open areas. The forest was significantly impacted by Hurricane Hugo in 1989, leading to a mixture of remnant large trees, natural regeneration, and approximately 1000 ha of planted pine. Forest management practices include prescribed fire and thinning to reduce wildfire risks and support longleaf pine

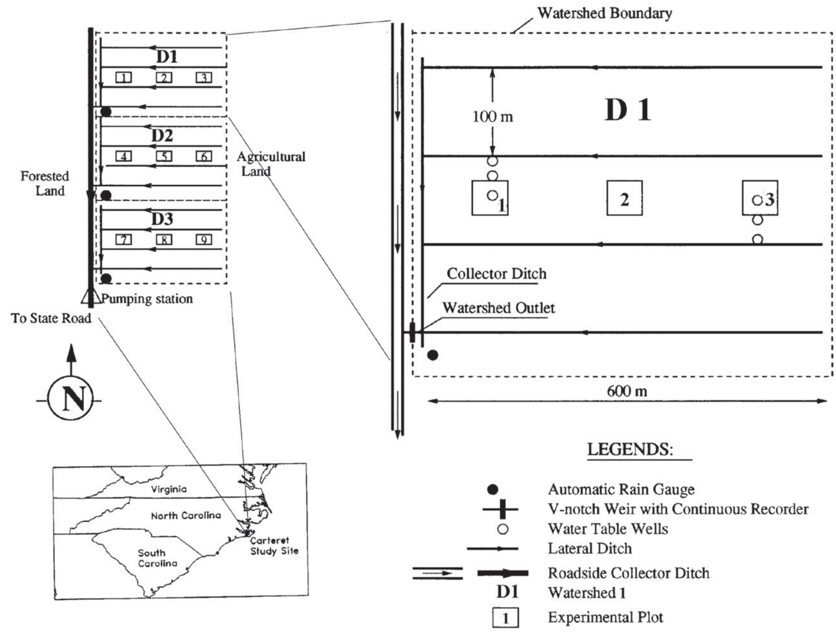

Figure 5. Location map of study watershed (D1) only, among two other adjacent watersheds D2 and D3, with hydrometeorological stations at the Carteret site in Coastal NC.

restoration and wildlife habitats, notably for the endangered red-cockaded woodpecker. For more details on WS78, please visit Amatya et al. (2024).

The sub-tropical climate of above three study sites on the coastal plain features hot, humid summers and moderate winters. Winters are wet due to low evapotranspiration (ET) and long-duration rain events, while summers have high ET demands and short-duration, high-intensity storms, including tropical storms in July and October.

The fourth study site is located in Carteret County, North Carolina, and is managed by Weyerhaeuser Company. The location map is given in Fig. 5. Three artificially drained experimental watersheds (D1, D2, and D3), each about 25 ha in size, were established in 1988 on a 14-year-old plantation. The site is flat with shallow water tables, and the soil is Deloss fine sandy loam, a hydric series. Each watershed is drained by four parallel lateral ditches, 1.4 to 1.8 m deep and spaced 100 m apart, which drain into a main roadside ditch via a collector ditch. The boundaries of the watersheds are defined by the mid-plane between the lateral ditches and rows of pine trees planted on 0.3 m high beds. Data on hydrology, soil, and vegetation parameters were collected from three experimental plots in each watershed. A detailed description of this watershed in NC can be found in Amatya and Skaggs (2011).

In our analysis, we focus on daily water table level prediction for all the above 4 study sites. We also conducted analyses of water table predictions on seasonal variations such as using monthly, growing, and dormant seasons for SC sites.

While data from 2004 to 2021 were used for the groundwater wells at WS77 and WS80, 2006 to 2019 for the wells at WS78 in SC, data from 1988 to 2008 was used for the well at D1 at the NC site. Detailed descriptions of data monitoring techniques including sensors and loggers and their accuracy and limitations are provided by Amatya et al. (2022) for the SC sites and by Amatya and Skaggs (2011) for the NC site.

4.2. Data collection, pre-processing, and EDA

While systematically compiling all the data at daily-aggregated levels before processing, several preprocessing steps were required, as shown below.

- There was missing data or data gaps for approximately 15–20 percent of all the data considered in the three watersheds. The data gaps can occur for different reasons. One of the reasons is power outage in weather stations running with batteries. If the batteries are out of work, it might take a few days to get that reported by the authorized person for checking periodically. In our study, we have omitted the dates completely with all data, even if one of the variables is missing. We did not do any missing data imputation.
- WS77 did not have a full weather station with daily variables such as solar radiation, wind speed, RH, etc. So these data was borrowed from the nearest station at WS78. However, daily flow data, water table, air temperature, soil temperature, and precipitation were available for WS77.
- For WS80 study site, weather data is available from 2011 only. So the weather data was borrowed from another nearest weather station SHQ site (see Fig. 4).
- Daily PET was estimated by the Priestley-Taylor method with the weather data from WS80 and WS78, and used for WS77 assuming they do not vary significantly. This is particularly because daily net radiation data was not available to calculate daily PET at each station.
- The net radiation for 2011–2019 was sometimes incomplete for the WS80 above the tree canopy tower. The Forest Service performed the missing data imputation. For the 2006–2010 period at the TC station on WS78, the unavailable daily net radiation was estimated using a relationship between daily solar vs net radiation between the TC and WS80 stations.
- For the WS78 site, net radiation was calculated using the measured solar radiation with the linear regression relationship between solar and net radiation for the WS80.
- Units of the variables used: for streamflow - mm, water table depth - cm, precipitation - mm, air and soil temperature - deg C, Relative humidity - %, solar and net radiation, Mj/sqm/day, Wind speed, m/sec; wind direction - deg, and vapor pressure deficit - kPa.
- As a pre-processing step, the covariates were normalized before being implemented in the model.

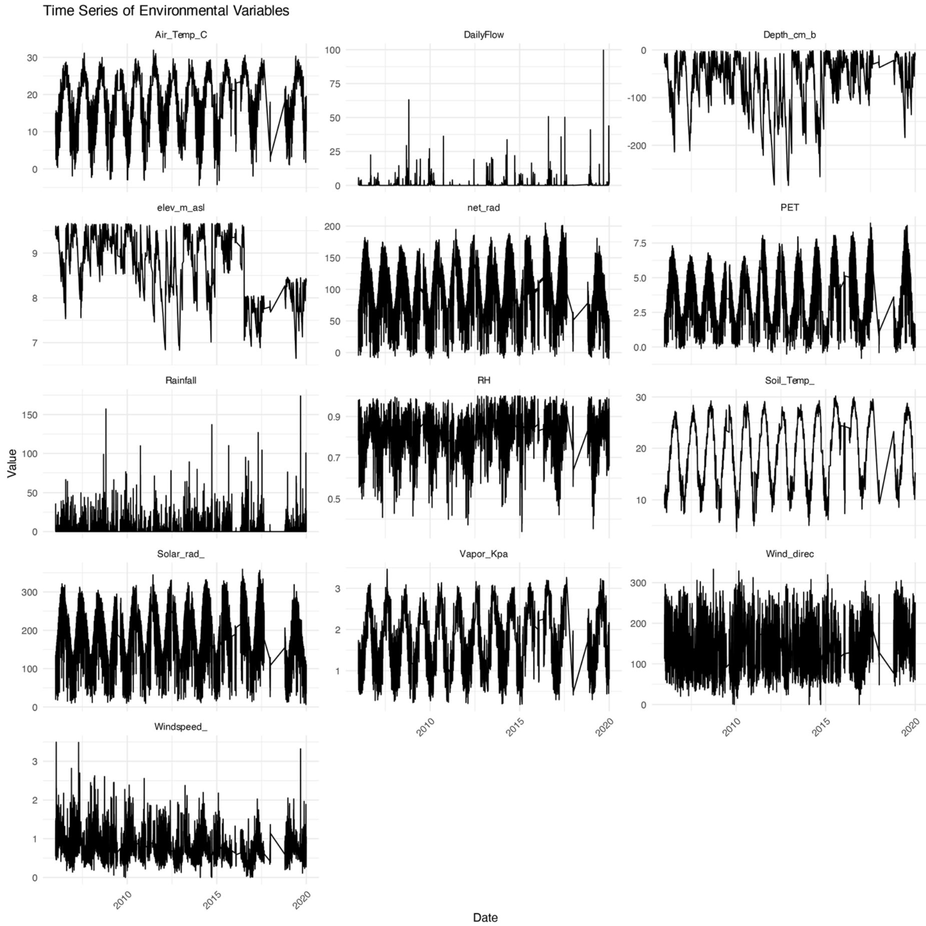

Figure 6. Weather variables daily time series plot used for water table depth prediction for WS77.

4.2.1. Exploratory data analysis

Figure 6 describes the different time series of weather data for WS77. Other watersheds demonstrate similar behavior of the autocorrelated variables. Figure 7 also demonstrates cross-correlation plot for different weather variables, which considers the lag of the different variables. A correlation plot is also given in the appendix for WS77, WS78, and WS80.

The plot shows variables are intercorrelated with each other. For example, air temperature is correlated with potential evapotranspiration (PET), net radiation, solar radiation, soil temperature, vapor pressure, etc. Soil temperature and solar radiation are two closely correlated variables, so their intercorrelation patterns with other variables are similar. PET is another weather variable correlated with rain, relative humidity, soil and air temperature, vapor pressure, and water table depth. Water table depth is correlated with air temperature, daily flow, net radiation, PET, rain, relative humidity, soil temperature, and other covariates.

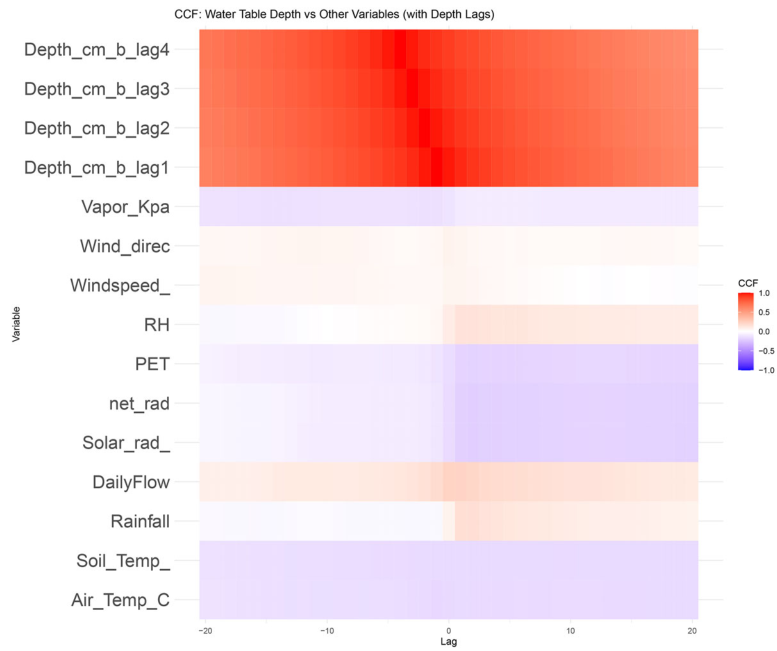

Figure 7. CCF for water table depth variables with the other weather variables across different lags for WS77.

Water table elevation represents the height of the water table in the soil profile relative to a (fixed) datum, while water table depth (WTD) is the position of the water table in the soil profile relative to the ground surface at the recording well, are well correlated. Therefore, we focused on water table depth (WTD), which is more commonly used in hydrology analysis.

Based on the exploratory data analysis and correlation plots, we hypothesize that a combination of climatic variables available at nearby weather stations could explain daily water table depth and elevation dynamics (fluctuations in terms of magnitude, duration, and frequency) at a given site. The primary challenge is to build a model that can predict daily water table depth under this complex setup, where various hydro-climatic variables are non-uniformly correlated with each other.

4.3. Final model selection and implementation

A time series model that handles an auto-regressive process in time series in the presence of different covariates with their lag structure is required for our analysis. The model can be explained below.

$$y_t = \nu + \sum_{\ell=1}^{p} \Phi^{(\ell)} y_{t-\ell} + \sum_{j=1}^{s} \boldsymbol{\beta}^{(j)} \mathbf{x}_{t-j} + u_t \quad \text{for} \quad t = 1, \ldots, T. \tag{1}$$

In this model, predictors are represented as $\{\mathbf{x}_t\}_{t=1}^{T}$, which are daily hydro-climatic variables, such as soil temperature, air temperature, precipitation, daily flow, wind speed, wind direction, relative humidity, solar radiation, net radiation, and potential evapotranspiration. Groundwater well depth measurements $\{\mathbf{y_t}\}_{t=1}^{T}$obtained from multiple wells at the study site are called the water table depth. The water table depth is used as dependent variables $\{\mathbf{y_t}\}_{t=1}^{T}$ for our other model. $\boldsymbol{\beta}^{(j)}$ is the coefficient vector of $\mathbf{x}_{t-j}$, j^{th} lag of the predictors and $\Phi^{(\ell)}$ is the l^{th} coefficient for the lag structure of y_t. An additive random Gaussian noise $u_t \overset{\text{wn}}{\sim} (0, \sigma_u^2)$ is considered in the model.

Elastic net combines LASSO and ridge penalties, allowing it to retain groups of correlated predictors while performing variable selection. This makes it more robust than LASSO alone when predictors exhibit high collinearity.

Let us define $\Phi := \left(\Phi^{(1)}, \Phi^{(2)}, \ldots, \Phi^{(p)}\right)$ as the vector of all coefficients of the lag structure of y_t with order p and $\boldsymbol{\beta} := \left(\boldsymbol{\beta}^{(1)}, \boldsymbol{\beta}^{(2)}, \ldots, \boldsymbol{\beta}^{(s)}\right)$ be the vector of coefficients of the predictors with their lag order s. For the variable selection, this method uses penalized regression with the least square loss function of 1 as $\lambda\left(\alpha\|[\Phi, \boldsymbol{\beta}]\|_1 + (1-\alpha)\|[\Phi, \boldsymbol{\beta}]\|_2^2\right)$, a method where all the coefficients are optimized over a smaller subset determined by $\lambda > 0$. The optimization function can be written as follows:

$$\min_{\nu, \Phi, \boldsymbol{\beta}} \sum_{t=1}^{T_1} \|y_t - \nu - \sum_{\ell=1}^{p} \Phi^{(\ell)} y_{t-\ell} - \sum_{j=1}^{s} \boldsymbol{\beta}^{(j)} \mathbf{x}_{t-j}\|^2 + \lambda\left(\alpha\|[\Phi, \boldsymbol{\beta}]\|_1 + (1-\alpha)\|[\Phi, \boldsymbol{\beta}]\|_2^2\right)$$

$0 \leq \alpha \leq 1$, is another parameter in the model which balances between the L_1 and L_2 norms of the coefficients. In general, for a vector $(x_1, x_2, \ldots, x_n)$, the L_2 norm is calculated by taking the square root of the sum of the squares of all the components:

$$\|\mathbf{x}\|_1 = |x_1| + |x_2| + \cdots + |x_n|, \|\mathbf{x}\|_2 = \sqrt{x_1^2 + x_2^2 + \cdots + x_n^2}.$$

L_1 Norm is the distance you walk in a grid-like city (Manhattan distance). One adds up the absolute values of the differences in each direction. L_2 Norm is the straight-line distance you would measure with a ruler (Euclidean distance). The Pythagorean theorem is used to calculate this distance. Both norms are useful in different contexts. The L_1 norm is often used when you want to emphasize sparsity (making many values zero), while the L_2 norm is used when the overall magnitude and smoothness are important factors to consider. Lasso tends to select only one variable from a group of highly correlated predictors, for example (in our case we can see in the supplementary material), which can lead to instability in the selected model when multiple predictors are equally important. Ridge tends to shrink the coefficients of correlated predictors together, but it doesn't perform variable selection i.e., it doesn't zero out coefficients. Elastic

Net strikes a balance between these two; it selects groups of correlated variables, unlike Lasso, and applies shrinkage like Ridge. This grouping effect is particularly useful when predictors are highly correlated, as it tends to select or exclude groups of related variables, leading to a more stable and interpretable model. Elastic Net allows for a weighted combination of both penalties. This flexibility can lead to better predictive performance, especially when neither Lasso nor Ridge alone is sufficient when there are many correlated features in high high-dimension setup.

The parameter λ is selected by the grid search within an interval of 10 to 500. The complete time series data range is from 1 to T which can be thought of as three segments. The first segment is 1 to T_1 which is commonly used as training data, the second segment is $T_1 + 1$ to T_2 which is used for parameter selection via cross-validation and the last segment is $T_2 + 1$ to T_3, a part of the time series of recent time, is used to evaluate the model performance. The period $T_1 + 1$ through T_2 is used to select λ. Define $\hat{y}_{\lambda,t+1}$ as the one-step ahead forecast based on $y_1, \ldots, y_t$. λ is chosen based on minimizing the one-step ahead mean square forecast error (MSFE) over the training period $T_1 + 1$ to T_2:

$$\text{MSFE}(\lambda) = \frac{1}{T_2 - T_1 - 1} \sum_{t=T_1}^{T_2-1} \|\hat{y}_{\lambda,t+1} - y_{t+1}\|^2.$$

MSFE is calculated for a range of lambda values over a grid of values, and the best lambda is chosen by cross-validation corresponding to the minimum MSFE. The BigVAR package performs rolling cross-validation, which respects the temporal ordering of observations and avoids leakage from future to past. α is a trade-off between the lasso (least absolute shrinkage and selection operator) and ridge penalties in the elastic net structure between 0 and 1. The default value for α is $\frac{1}{k+1}$ where $k = 1$ in our case. It means we are taking equal weight of the lasso and ridge penalty in the penalization. The combination of the Lasso and ridge penalty is considered in this time series analysis method to improve the prediction accuracy for the ridge and interpretability of regression models for the lasso and ridge. The prediction of horizon 1 which is 1 day ahead of prediction in recent time is considered as testing data. σ_u^2 is unknown, so updated until convergence during the optimization procedure.

For the daily water table depth prediction, we used all the daily data for three of the watersheds in SC and D1 in NC. While doing the seasonal variants, for dormant season, we filtered the daily data only for the dormant season for each year and followed the similar procedure described above. For growing season, we filtered the daily level growing data for each of the year and followed similar modeling procedure. For the monthly prediction, we used the total amount of rainfall and average of remaining variables for each month of the years from the daily available watershed data. Although we do not recommend using the monthly average data for prediction in practice due to huge variability in different weather variables from their mean, we only show the performance in the tables.

The testing period of this model T_1+1 through T_2 with the default L_2 loss and horizon as 1, an interval where $T_1 = \lfloor \frac{T}{3} \rfloor$ and $T_2 = \lfloor \frac{2T}{3} \rfloor$ and presented all the residual performance in the model which fits the least square. The parameters are described in the supplement material.

In Fig. 7, we encountered that generally water table depth is highly dependent on the 4 previous day's lag. The dependence between covariates becomes weaker at higher lags. Hence, for the lag structure, we have used $p = 4$ as the lag of water table depth and $s = 2$ as the lag of different hydro-climatic variables that we use for inference as the maximum values. The final values of p and s were selected based on the Bayesian Information Criterion (BIC), which combines the goodness of fit and the complexity into a single number. The Bayesian Information Criterion (BIC) is defined as:

$$\text{BIC} = -2\log(\hat{L}) + k\log(n)$$

where $\hat{L}$ is the maximum likelihood of the model, k is the number of parameters in the model, and n is the number of data points. we compare our results based on the following metrics. Let y_i be the actual value, $\hat{y}_i$ be the predicted value, $\bar{y}$ be the mean of the actual values, n is the number of observations, and p is the number of predictors. Then the definitions of R^2, adjusted R^2, Mean Squared Error (MSE), and Root Mean Squared Error (RMSE) are defined below which we use as a comparison metric in different models and scenarios.

$$R^2 = 1 - \frac{\sum_{i=1}^{n}(y_i - \hat{y}_i)^2}{\sum_{i=1}^{n}(y_i - \bar{y})^2}, \qquad \text{adjusted } R^2 = 1 - \frac{(1-R^2)(n-1)}{n-p-1}$$

$$\text{MSE} = \frac{1}{n}\sum_{i=1}^{n}(y_i - \hat{y}_i)^2, \qquad \text{RMSE} = \sqrt{\frac{1}{n}\sum_{i=1}^{n}(y_i - \hat{y}_i)^2}.$$

The Nash–Sutcliffe efficiency is equivalent to the coefficient of determination (R^2), thus ranging between $-\infty$ and 1.

Mean Error (ME) measures the bias of the model; how much the average predicted value deviates from the observed. Can be positive or negative, indicating over- or under-prediction. Mean Absolute Error (MAE) is the average absolute difference between predicted and observed values. It is easier to interpret since its in the same units as the data. Mean Squared Error (MSE) is the average of squared differences between predicted and observed values, emphasizing larger errors due to the squaring. Root Mean Square Error (RMSE) is the square root of MSE; in the same units as the data, emphasizing larger errors more than MAE.

Unbiased Root Mean Square Error (ubRMSE) is similar with RMSE, but without bias. It isolates random error by removing systematic error (bias). Normalized RMSE (NRMSE) is normalized by the range or mean of the observed data, allowing comparison across different datasets. Percent Bias (PBIAS) shows the average tendency of predictions to over or under predict. A negative value indicates model overestimation. Ratio of RMSE to Standard Deviation (RSR) is a ratio of RMSE to the standard deviation of observed data. Low RSR indicates better model performance. Ratio of Standard Deviations (rSD) compares variability between predicted and observed values. A value near 1 indicates similar variability. The lower limit of NSE is $-\infty$, so to eliminate this problem $\text{NNSE} := \frac{1}{2-\text{NSE}}$.

Modified NSE (mNSE) modifies NSE to address issues with extreme values. Relative NSE (rNSE) considers relative differences between predictions and observations. Weighted NSE (wNSE) is a NSE variant that gives different weights to data points, often used for hydrological predictions. Weighted Seasonal NSE (wsNSE) is another NSE modified to account for seasonal effects, useful for predicting seasonal dynamics. Index of Agreement (d) measures agreement between predictions and observations. It ranges from 0 to 1, with 1 indicating perfect agreement. Refined Index of Agreement (dr) addresses the limitations of the original index of agreement. Modified Index of Agreement (md) is a variation of the index of agreement that better addresses certain model behaviors. Relative Index of Agreement (rd) is a relative measure of agreement between predictions and observations. Persistence Index (cp) is a measure that evaluates how persistent the predicted signal is compared to the observed. Pearson Correlation Coefficient (r) measures the linear relationship between predicted and observed values. "r" range from -1 (perfect negative correlation) to 1 (perfect positive correlation). Coefficient of Determination (R^2) represents the proportion of variance explained by the model. A value closer to 1 indicates a good fit.

Volumetric Efficiency (VE) evaluates how well the model reproduces total volume of observed data, often used in hydrological models. Kling-Gupta Efficiency (KGE) combines correlation, bias, and variability to give a more holistic measure of model performance than NSE. KGE for Low Values (KGElf) is a version of KGE that gives more weight to low values in predictions, useful in low-flow regimes. Non-parametric KGE (KGEnp) is A non-parametric version of KGE, often more robust against outliers. We have applied the above metric to evaluate the performance of our model.

5. Software and data availability

"BigVAR" (Nicholson, Matteson, and Bien 2017) is an existing R Package designed to handle high-dimensional multivariate time series modeling using vector autoregressions (VAR). It provides efficient methods for estimating VAR models when the number of variables is large relative to the number of periods, which is common in many modern applications. The package focuses on overcoming the challenges of overfitting in such high-dimensional settings by incorporating various regularization techniques. The R package is available for this model (Nicholson, Matteson, and Bien 2019). For further references see BigVAR implementation in R. Our codes for analysis and application are available in GitHub.

- We used the software available here http://www.wbnicholson.com/BigVAR.html. The detailed documentation is also available here.
- Program language: R.
- Our developed code for inference is available at https://github.com/alokesh17/Water_Table_Depth-.git.
- The data for three study sites WS77, WS78, and WS80 located at the US Forest Service Santee Experimental Forest/Center for Forested Wetlands in https://www.fs.usda.gov/rds/archive/Catalog/RDS-2019-0033.

6. Guidelines for practitioners

The details of the guidelines for the practitioners are kept in the supplementary material. It includes data preparation, seasonal filtering, model fitting with parameter settings, and finally, the prediction.

Remark 1. To demonstrate the practical utility of our forecasting framework, consider a forested wetland where maintaining optimal water table depth is essential for sustaining native vegetation and minimizing drought-induced ecosystem degradation. Using the proposed autoregressive, hydroclimatic predictor–driven model, managers can generate short-term (e.g., 1–15 day horizon) forecasts of water table depth under baseline climatic conditions as well as scenario-based simulations incorporating anticipated drought, increased precipitation, or planned hydrological interventions such as controlled inflow or drainage. These forecasts may be compared against predefined ecological thresholds—for instance, triggering re-wetting efforts when projected water tables are predicted to drop below a critical depth for multiple consecutive days. By integrating model outputs with real-time monitoring networks and updating forecasts as new observations become available, the approach supports an adaptive management cycle in which interventions are scheduled proactively, resource allocation is optimized, and ecological risk associated with hydrological extremes is reduced. This case study illustrates how model-based prediction can move beyond retrospective analysis to directly inform evidence-based wetland management decisions.

7. Residual diagnostics and model fit assessment

In this section, we discussed different time series plots and residual analysis for watersheds. Then further we demonstrate the variable selection, exploration without daily flow variable and data assimilation for out-of-sample prediction with a bigger horizon of 14 days.

7.1. Time series plots

In the Figs. 8 and 9, the actual vs prediction of water table depth for three different watersheds from South Carolina WS77, WS78, WS80, and one watershed D1 from North Carolina over time series for a daily-level prediction is plotted. The actual measurement is represented by a cross symbol ($\times$), while the predicted measurement is denoted by a delta symbol (Δ).

In the graph of the depths of the water table of 2017 for WS80 in SC and the year 2007, D1 in NC in Fig. 10 to obtain a clear picture of our prediction for a

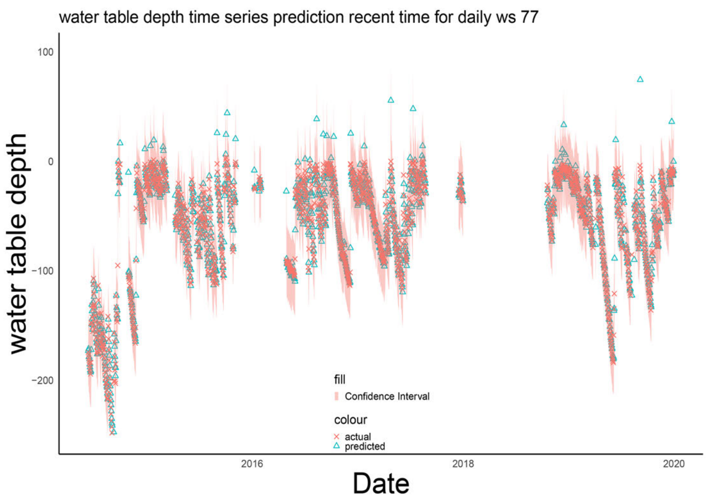

(a) Time series for ws77

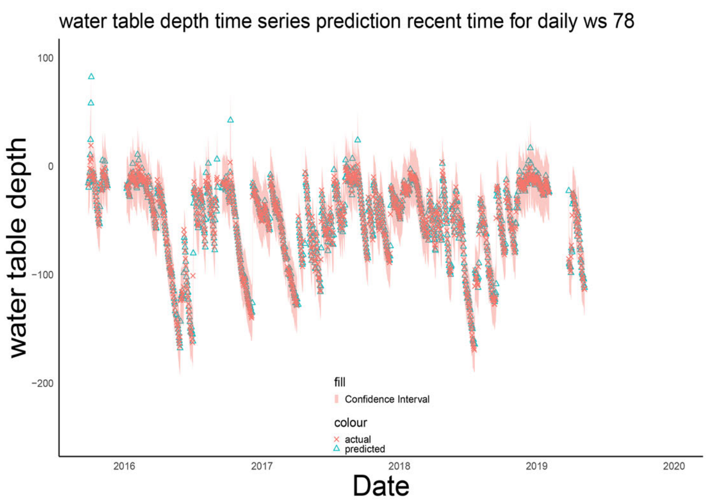

(b) Time series for WS78

Figure 8. Time series of predicted versus measured daily water table depths in cm, including their 95% confidence intervals (hatched area), for the wells at (a) ws77 and (b) ws78 during the 2016–2019 testing period. The plots highlight the model's ability to track short-term fluctuations in water table depth, with 95% confidence intervals indicating prediction uncertainty.

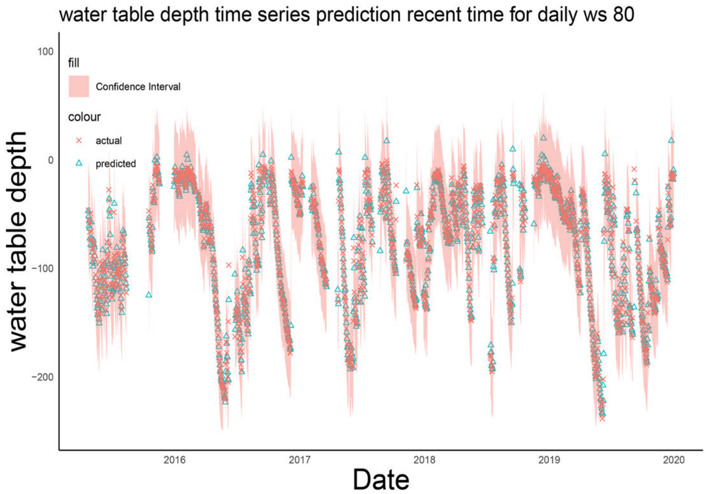

(a)

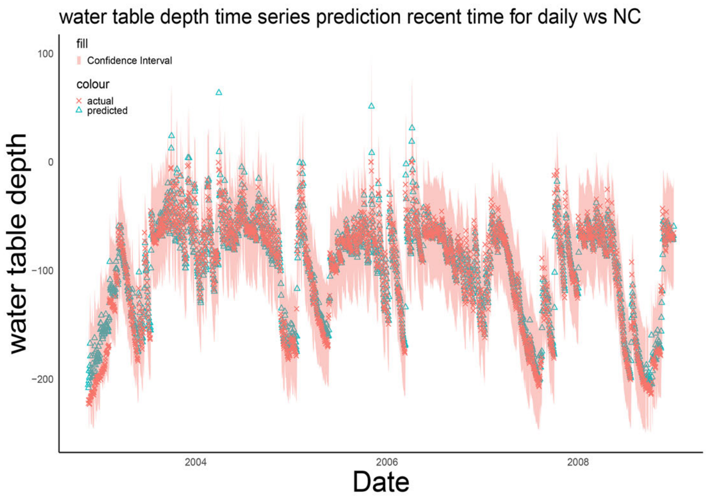

(b)

Figure 9. Time series of Predicted versus measured daily water table depths in cm including their 95% confidence intervals (hatched area) for the wells (a) at WS80 for the 2016–2019 and (b) D1 in NC for the 2004–2008 testing period. The plots highlight the model's ability to track short-term fluctuations in water table depth, with 95% confidence intervals indicating prediction uncertainty.

very dry year and 2016 for WS80 in SC and the year 2005, D1 in NC in Fig. 11 to obtain a clear picture of our prediction for a relatively wet year. The actual versus predicted plot for three different well locations in WS77 and WS78 in SC and one in watershed D1 in NC is shown in Fig. 12. The model achieved an R^2 0.93 for 2019 (dry year) and 0.96 for 2016 (wet year) for WS80 which demonstrates the model's performance is robust in extreme hydrological conditions. The climate conditions for WS77 and WS78 are similar as WS80. For another well D1 in

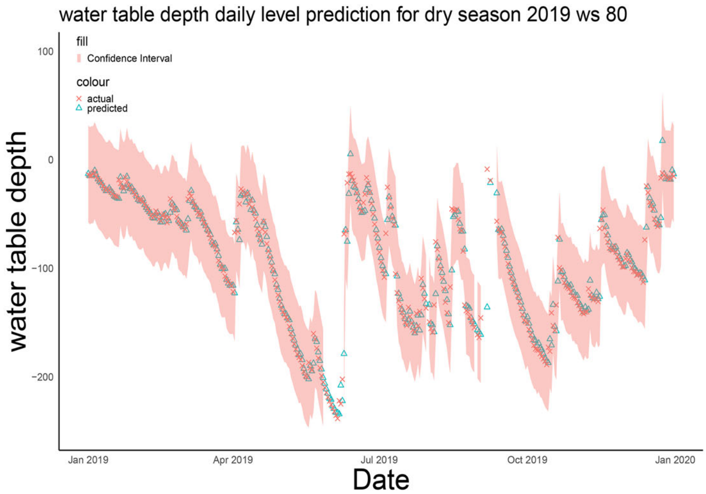

(a)

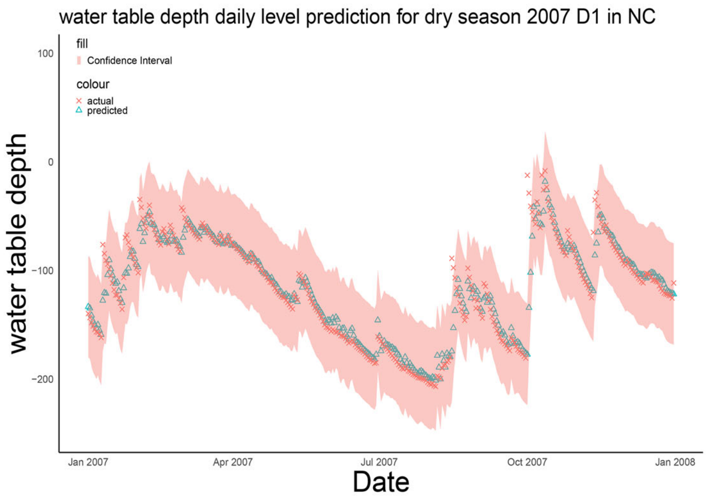

(b)

Figure 10. Time series plots of predicted vs measured in cm for dry year 2019 WS80 in SC and 2007 D1 in NC. The plots highlight the model's ability to track short-term fluctuations in water table depth, with 95% confidence intervals indicating prediction uncertainty.

North Carolina, the extreme weather condition results are also accurate, with a higher confidence interval width compared with the wells is SC.

The total training period is considered 1 to T_2 time interval and the testing interval is $T_2 + 1$ through T with the horizon as 1. A point estimate gives only a single value as the best estimate of the population parameter. However, a confidence interval provides a range of plausible values for that parameter, giving a better understanding of the uncertainty associated with the estimate (see Manna et al. 2024). A prediction interval is included, where $\mathrm{SE} = \sqrt{\sum_{t=T_2+1}^{T} (y_t - \hat{y}_t)^2}$

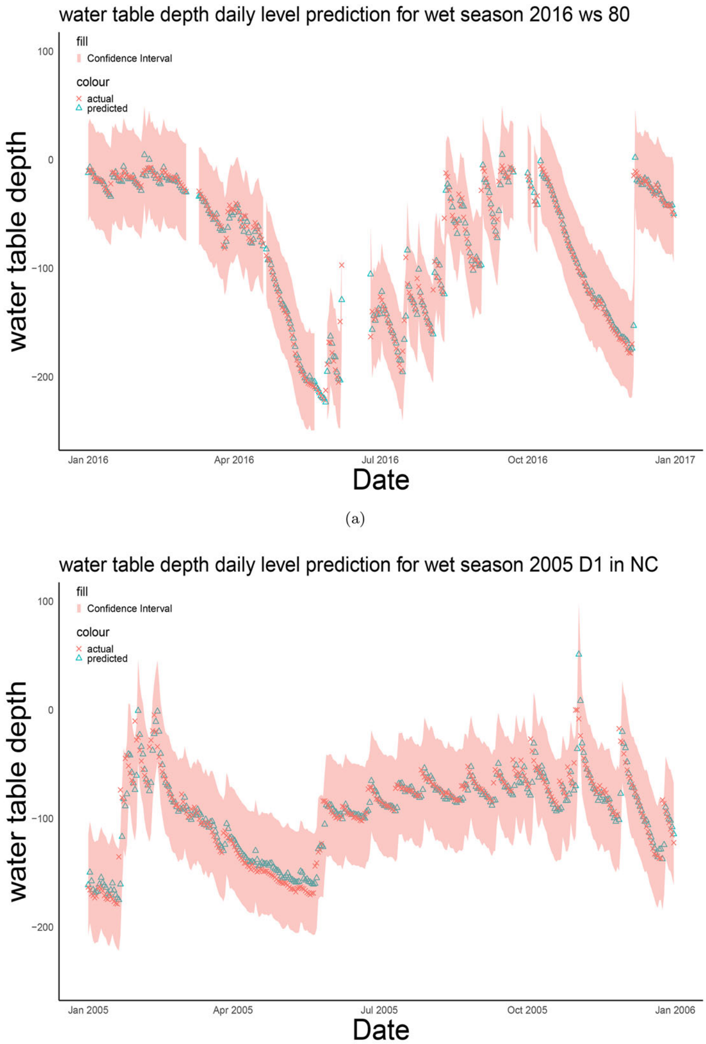

(a)

(b)

Figure 11. Time series plots of predicted vs measured in cm for wet year 2016 WS80 in SC and 2005 D1 in NC. The plots highlight the model's ability to track short-term fluctuations in water table depth, with 95% confidence intervals indicating prediction uncertainty.

as

$$\left(\hat{y}_t - 3\text{SE}, \hat{y}_t + 3\text{SE}\right); t = T_2 + 1, \cdots, T.$$

A table describing the performance of proposed model for daily level in SC WS data is given in Table 1. Another table is presented with the performance of proposed model for SC WS data in a few other seasonal variants in Table 2. A detailed analysis of goodness of fit measures based on the "HydroGof" package (see Zambrano-Bigiarini 2017) for different seasonal variation comparisons are provided in Tables 3 and 4.

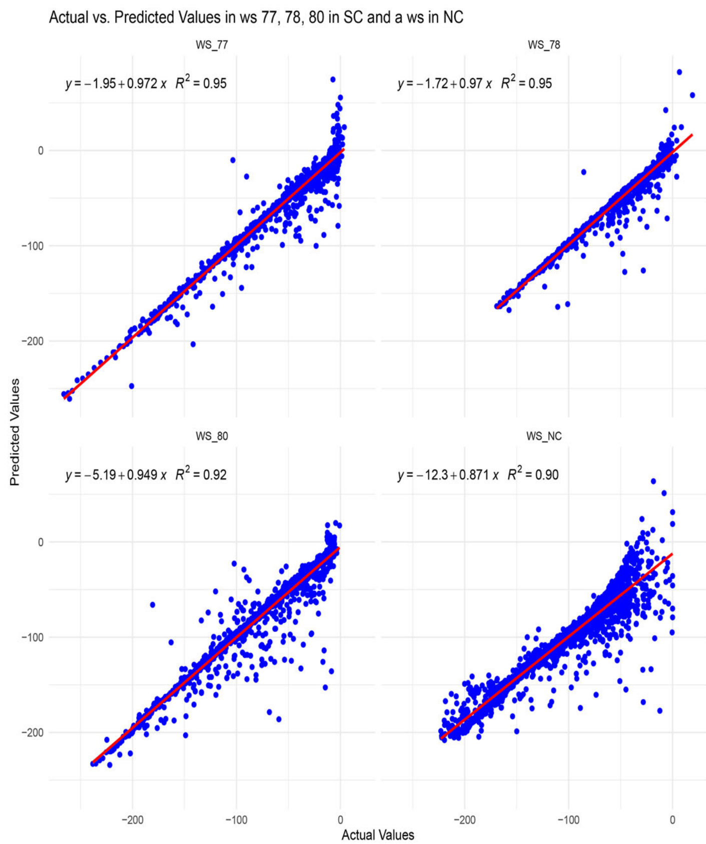

(a)

Figure 12. Scatter plots of predicted and measured daily water table depths in cm for watersheds WS77, WS78, WS80 in SC and D1 in NC. The residual plot can be found in the appendix.

Table 1. Residual analysis for water table depth at daily level.

well on Watershed	Reg line (y=)	adj R sq	MSE	RMSE	Nash-Sutcliffe efficiency
WS77	−0.82 + 0.98x	0.95	116.37	10.79	0.95
WS78	−1.00 + 0.97x	0.94	75.13	8.67	0.95
WS80	−0.86 + 0.97x	0.92	223.28	14.94	0.92
D1	−3.05 + 1.03x	0.90	242.39	15.57	0.90

Notes: In Reg line, *y* is actual, and *x* is predicted. MSE is measured in sq cm.

The following tables provide a detailed analysis of residual metrics for water table depth across different seasonal conditions and years. Note that monthly is the monthly temporal scale by averaging all daily values to monthly whereas seasonal is using daily values for each of the growing seasons (not the daily values averaged for each growing season, e.g. two values per year). In the first table (Table 3), coefficients are presented for several performance metrics across multiple periods. For instance, ME (Mean Error) varies notably between different seasonal conditions and years, for example, 0.61 in WS77_dormant. MAE (Mean Absolute Error) shows considerable differences as well, with WS80_daily

Table 2. Residual analysis for water table depth for SC monthly, growing, and dormant season.

Watershed	adj R sq	MSE	RMSE	Nash-Sutcliffe Efficiency
WS77 Monthly	0.14	922.94	30.38	0.14
WS77 Growing	0.93	164.86	12.84	0.93
WS77 Dormant	0.93	74.88	8.65	0.93
WS78 Monthly	0.56	489.50	22.12	0.56
WS78 Growing	0.90	63.11	7.94	0.90
WS78 Dormant	0.89	50.56	7.11	0.89
WS80 Monthly	0.16	1479.47	38.46	0.16
WS80 Growing	0.90	304.14	17.44	0.90
WS80 Dormant	0.94	101.81	10.09	0.94

Note: MSE is measured in sq cm.

Table 3. Detailed Residual analysis for water table depth for SC monthly, growing and dormant season part 1.

	WS77_daily	WS77_monthly	WS77_growing	WS77_dormant	WS78_daily	WS78_monthly
ME	0.29	−0.03	0.29	0.61	0.19	−3.67
MAE	5.52	23.93	6.91	4.08	4.06	18.54
MSE	116.37	922.94	164.86	74.88	75.13	489.50
RMSE	10.79	30.38	12.84	8.65	8.67	22.12
ubRMSE	10.78	30.38	12.84	8.63	8.67	21.82
NRMSE %	21.80	91.60	25.60	26.40	23.20	65.40
PBIAS %	−0.50	0.10	−0.40	−1.60	−0.40	7.40
RSR	0.22	0.92	0.26	0.26	0.23	0.65
rSD	1.00	0.80	1.02	1.01	1.00	0.83
NSE	0.95	0.14	0.93	0.93	0.95	0.56
mNSE	0.86	0.06	0.82	0.83	0.86	0.32
rNSE	−39.43	−0.81	−1.14	−8.68	0.54	−11.02
wNSE	0.98	−0.27	0.97	0.96	0.96	0.55
d	0.99	0.70	0.98	0.98	0.99	0.85
dr	0.93	0.53	0.91	0.92	0.93	0.66
md	0.93	0.48	0.91	0.92	0.93	0.62
rd	−9.14	0.36	0.47	−1.42	0.89	−3.02
cp	0.51	0.42	0.48	0.38	0.36	0.47
r	0.98	0.49	0.97	0.97	0.97	0.76
R2	0.95	0.14	0.93	0.93	0.95	0.56
bR2	0.94	0.11	0.93	0.91	0.94	0.52
KGE	0.98	0.45	0.96	0.96	0.97	0.70
KGElf	−1.77	0.02	−9.56	0.37	0.19	−44.23
KGEnp	0.96	0.47	0.95	0.94	0.97	0.75
VE	1.09	1.45	1.10	1.11	1.08	1.38

Note: MSE is measured in sq cm.

exhibiting the highest value of 8.88, contrasting with the lowest value of 4.06 in WS78_daily.

Meanwhile, metrics like MSE (Mean Squared Error) and RMSE (Root Mean Squared Error) reflect the variability in model accuracy across different conditions. For example, WS77_growing during generally wet season shows the MSE 164.86 and RMSE of 12.84, whereas WS77_dormant shows the MSE of 74.88 and RMSE of 8.65, indicating better model performance during dormant periods with less evaporative demand. Table 2 presents a detailed comparison of residual metrics for water table depth across different seasonal conditions (growing and dormant) in various watersheds (WS77, WS78, WS80).

Table 4. Detailed Residual analysis for water table depth for SC sites monthly, growing and dormant season part 2.

	WS78_growing	WS78_dormant	WS80_daily	WS80_monthly	WS80_growing	WS80_dormant
ME	−1.49	−0.18	1.24	7.74	1.30	1.22
MAE	4.86	3.26	6.95	31.29	8.88	4.48
MSE	63.11	50.56	223.28	1479.47	304.14	101.81
RMSE	7.94	7.11	14.94	38.46	17.44	10.09
ubRMSE	7.80	7.11	14.89	37.68	17.39	10.02
NRMSE %	31.60	32.70	28.10	90.50	31.60	24.50
PBIAS %	2.30	0.60	−1.60	−9.20	−1.40	−2.20
RSR	0.32	0.33	0.28	0.91	0.32	0.24
rSD	1.04	0.99	1.01	1.00	1.03	1.01
NSE	0.90	0.89	0.92	0.16	0.90	0.94
mNSE	0.77	0.81	0.84	0.03	0.81	0.87
rNSE	0.90	0.44	−2.46	−0.76	0.63	0.25
wNSE	0.89	0.94	0.92	−0.10	0.90	0.93
d	0.98	0.97	0.98	0.76	0.98	0.99
dr	0.88	0.91	0.92	0.52	0.91	0.93
md	0.89	0.91	0.92	0.55	0.91	0.93
rd	0.98	0.86	0.14	0.51	0.91	0.81
cp	0.39	0.27	0.25	0.03	0.31	0.18
r	0.95	0.95	0.96	0.60	0.95	0.97
R2	0.90	0.89	0.92	0.16	0.90	0.94
bR2	0.88	0.88	0.90	0.14	0.89	0.92
KGE	0.93	0.95	0.96	0.59	0.94	0.96
KGElf	0.93	0.36	0.39	−0.06	0.38	0.53
KGEnp	0.94	0.96	0.95	0.52	0.94	0.96
VE	1.08	1.11	1.09	1.37	1.10	1.08

Note: MSE is measured in sq cm.

For WS77, the model's adjusted R-squared values vary significantly across seasons: growing (0.93), and dormant (0.93). Correspondingly, the Mean Squared Error (MSE) ranges from 164.86 (growing) to 74.88 (dormant), reflecting differing levels of model accuracy. Root Mean Squared Error (RMSE) follows a similar trend, with values ranging from 12.84 (growing) to 8.65 (dormant), indicating higher precision during dormant periods.

In WS78, the adjusted R-squared values are moderately high across all seasons: growing (0.90), and dormant (0.89). The MSE decreases notably from 63.11 (growing) to 50.56 (dormant), suggesting improved model performance during dormant periods. RMSE also decreases accordingly, with values ranging from 7.94 (growing) to 7.11 (dormant).

For WS80, the model's adjusted R-squared values show some variation: growing (0.90), and dormant (0.94). The MSE is highest in the growing period (304.14) and lowest during the dormant season (101.81), indicating varying levels of accuracy. RMSE values range from 17.44 (growing) to 10.09 (dormant), illustrating the model's ability to predict more accurately during dormant conditions.

NRMSE is lower during the dormant period for WS80, indicating better model performance during this phase. The growing season has the highest NRMSE, particularly for WS78 and WS80, indicating more variability in predictions during that period. NSE values are consistently high across all sites and periods with the daily showing slightly higher efficiency values compared to dormant and growing seasons. The weighted NSE, like the standard NSE, shows higher values during the daily period.

These metrics provide insights into the performance and variability of water table depth predictions across different environmental contexts, aiding in better understanding and management of water resources in agricultural and environmental applications.

7.2. Variable selection

Variable selection allows researchers to identify the most relevant variables to include in a model, leading to improved model performance, better interpretability, and reduced overfitting by eliminating unnecessary variables that could introduce noise and complexity to the analysis. In this section, we are demonstrating the important variables which are sufficient for a practitioner to build a daily water table predictive model.

In the Table 5 (the corresponding tables for WS78 and WS80 is in the supplementary material), the coefficients of the models for water table depth for three different watersheds with four different time setups are provided. In this model, elastic net, a penalization over the coefficients approach, is used for inference. If a coefficient is closer to zero, the corresponding variable is less sensitive than the other variables away from zero. The table "Coefficients of WS77" presents regression coefficients for various models applied to Watershed 77 (WS77).

These models predicted a dependent variable based on multiple independent variables. Each column represents a different time scale or season: daily, monthly, growing season, and dormant season. The intercept is the constant term in the regression equation. It represents the expected value of the dependent variable when all predictors are zero. Y1L1, Y1L2, Y1L3, and Y1L4 are lagged values of the dependent variable. These coefficients indicate the influence of previous values of the dependent variable on the current value. Air_Temp_C1 is the coefficient for air temperature at time lag 1 and Air_Temp_C2 is the coefficient for air temperature at time lag 2. This notation applies to each of the other variables. This table illustrates how the influence of various factors on the dependent variable differs across daily, monthly, growing season, and dormant season periods. Zero values indicate that the corresponding variable was not included in the model for the specific period.

For the intercepts: WS77_daily: −0.605, WS77_growing: −0.818, WS77_dormant: 3.842 Among the predictors, notable differences across conditions are observed: Y1L1 has consistent positive coefficients across all conditions, ranging approximately from 0.573 to 0.945.

Rainfall1 shows variations, with coefficients of approximately 0.459 for WS77_daily, 0.505 for WS77_growing and around 0.462 for WS77_dormant.

Table 5. Coefficients of WS77.

	WS77_daily	WS77_monthly	WS77_growing	WS77_dormant
intercept	−0.60460214	−44.17051465	−0.81780409	3.84158477
Y1L1	0.94170219	0.57386687	0.92943288	0.94451563
Y1L2	0.00000000	−0.06360627	0.00000000	0.02414715
Y1L3	0.00000000	0.06150226	0.00000000	0.00000000
Y1L4	0.02612793	−0.07874109	0.02473702	0.01099902
Air_Temp_C1	0.00000000	0.22590743	0.00000000	0.00000000
Soil_Temp_1	0.00000000	0.00000000	0.00000000	0.00000000
Rainfall1	0.45885660	0.00000000	0.50514104	0.46214280
DailyFlow1	−0.10814269	−0.03207597	−0.47766625	−0.04136039
Solar_rad_1	−0.03770686	0.00000000	−0.03914593	−0.03038076
net_rad1	0.00000000	0.00000000	0.00000000	0.00000000
PET1	0.00000000	0.00000000	0.00000000	0.00000000
RH1	0.00000000	0.00000000	0.00000000	0.00000000
Windspeed_1	0.00000000	−0.04562469	0.00000000	0.00000000
Wind_direc1	−0.00119424	0.00000000	0.00885937	−0.01274562
Vapor_Kpa1	0.00000000	0.25763440	0.00000000	0.00000000
Air_Temp_C2	0.00000000	0.00000000	0.00000000	0.00000000
Soil_Temp_2	0.00000000	−0.99438617	0.00000000	0.00000000
Rainfall2	0.00000000	−0.80569544	0.00957783	0.00000000
DailyFlow2	0.00000000	−0.28049803	0.03664337	0.01046831
Solar_rad_2	0.01681527	0.00000000	0.01030524	0.00143884
net_rad2	0.00000000	0.00000000	0.00000000	0.00000000
PET2	0.00000000	0.00000000	0.00000000	0.00000000
RH2	0.00000000	0.00000000	0.00000000	0.00000000
Windspeed_2	0.00000000	0.29262960	0.00000000	0.00000000
Wind_direc2	0.00363181	0.00000000	0.00063054	−0.00263301
Vapor_Kpa2	0.00000000	0.16987948	0.00000000	0.00000000

Note: The tables for WS78 and WS80 are in the supplement.

DailyFlow1 has negative coefficients, ranging from −0.032 to −0.478, with WS77_growing exhibiting the most negative impact. Wind direction with 2nd order lag might have some small influence except the monthly prediction. Certain predictors such as Air_Temp_C1, Soil_Temp_1, net_rad1, PET1, and RH1 have coefficients of zero across all conditions, indicating no significant impact in these scenarios. Similar patterns are observed in other predictors across different conditions, reflecting their varying degrees of influence.

In summary, the coefficients vary widely across the different conditions of WS77_daily, WS77_growing, and WS77_dormant, underscoring the nuanced relationships between predictors and outcomes in each specific context. These variations highlight the importance of considering environmental and growth conditions when interpreting the effects of predictors on the response variable. For the other two watersheds in SC, WS77 and WS78 a similar pattern of important coefficients are observable.

With BigVAR's elastic-net penalty, variable importance is inferred from which lagged predictors receive non-zero coefficients, reflecting automatic feature selection. Because shrinkage biases effect sizes, interpretability requires post-selection refitting or analysis of regularization paths (Manna et al. 2024, 2025c, 2025b, e.t.c.).

7.3. Exploration without daily-flow variable

In Sec. 7.2, we observed that daily flow with its one and two days lag is important for WS77 and WS78 water table depth prediction.

The investigation how the prediction might have changed if the daily flow variable is absent is also important as daily flow data is not frequently available like other climatic parameters. The coefficients are described in Table 6 (the corresponding tables for WS78 and WS80 are in the supplementary material) for three different stations in SC.

The residuals are listed in Tables 7 and 8. The set of important coefficients did not change significantly. In terms of daily level prediction, the mean squared error (MSE) for WS77 changed from 116.37 to 116.81, for WS78 changed from 75.13 to 75.68, and for WS80 almost no change was observed. For monthly prediction, the MSE for WS77 changed from 922.94 to 936.28, for WS78 changed from 489.50 to 326.32, and for WS80 almost no change was observed.

During the growing period, the MSE for WS77 changed from 164.86 to 201.49, for WS78 changed from 63.11 to 63.30, and for WS80 almost no change was observed. During the dormant period, the MSE for WS77 changed from 74.88 to 82.44, and for WS78 and WS80, almost no change was observed. Hence, dropping the daily-flow variable did not result in a significant change in the model prediction.

Table 6. Coefficients of WS77 without daily-flow variable.

	WS77_daily	WS77_monthly	WS77_growing	WS77_dormant
intercept	−0.85632733	−44.72741826	0.09830566	2.79063069
Y1L1	0.93853701	0.57162827	0.97742642	0.94503564
Y1L2	0.00000000	−0.06954435	−0.03778470	0.01449843
Y1L3	0.00000000	0.06535313	0.00000000	0.00000000
Y1L4	0.02807640	−0.07969383	0.01013189	0.01495053
Air_Temp_C1	0.00000000	0.24341318	0.00000000	0.00000000
Soil_Temp_1	0.00000000	0.00000000	0.00000000	0.00000000
Rainfall1	0.45628644	−0.03634609	0.30991193	0.37887521
Solar_rad_1	−0.03762190	0.00000000	−0.04888764	−0.03384639
net_rad1	0.00000000	0.00000000	0.00000000	0.00000000
PET1	0.00000000	0.00000000	0.00000000	0.00000000
RH1	0.00000000	0.00000000	0.00000000	0.00000000
Windspeed_1	0.00000000	−0.04789414	0.00000000	0.00000000
Wind_direc1	−0.00154098	0.00000000	0.01031562	−0.01391166
Vapor_Kpa1	0.00000000	0.25786024	0.00000000	0.00000000
Air_Temp_C2	0.00000000	0.00000000	0.00000000	0.00000000
Soil_Temp_2	0.00000000	−1.00013527	0.00000000	0.00000000
Rainfall2	0.00000000	−0.27353078	−0.07273526	0.00000000
Solar_rad_2	0.01727760	0.00000000	0.01592106	0.00830007
net_rad2	0.00000000	0.00000000	0.00000000	0.00000000
PET2	0.00000000	0.00000000	0.00000000	0.00000000
RH2	0.00000000	0.00000000	0.00000000	0.00000000
Windspeed_2	0.00000000	0.29280204	0.00000000	0.00000000
Wind_direc2	0.00393818	0.00000000	0.00257751	−0.00117845
Vapor_Kpa2	0.00000000	0.16120519	0.00000000	0.00000000

Note: The tables for WS78 and WS80 are in the supplement.

Table 7. Detailed Residual analysis for water table depth for SC monthly, growing and dormant season without daily-flow variable part 1.

	WS77_daily	WS77_monthly	WS77_growing	WS77_dormant	WS78_daily	WS78_monthly
ME	0.29	0.02	0.17	0.55	0.18	−2.56
MAE	5.52	24.17	7.37	4.18	4.07	15.04
MSE	116.81	936.38	201.49	82.44	75.68	326.32
RMSE	10.81	30.60	14.19	9.08	8.70	18.06
ubRMSE	10.80	30.60	14.19	9.06	8.70	17.88
NRMSE %	21.90	92.00	28.10	27.40	23.20	59.30
PBIAS %	−0.50	−0.00	−0.30	−1.50	−0.30	5.10
RSR	0.22	0.92	0.28	0.27	0.23	0.59
rSD	1.00	0.80	1.01	1.00	1.00	0.93
NSE	0.95	0.13	0.92	0.92	0.95	0.64
mNSE	0.86	0.05	0.81	0.83	0.86	0.41
rNSE	−86.44	−0.86	0.53	−0.66	0.55	−1.36
wNSE	0.98	−0.28	0.98	0.96	0.96	0.60
d	0.99	0.69	0.98	0.98	0.99	0.89
dr	0.93	0.52	0.90	0.92	0.93	0.70
md	0.93	0.48	0.90	0.92	0.93	0.68
rd	−20.94	0.34	0.88	0.58	0.89	0.30
cp	0.51	0.41	0.43	0.36	0.35	0.54
r	0.98	0.48	0.96	0.96	0.97	0.81
R2	0.95	0.13	0.92	0.92	0.95	0.64
bR2	0.94	0.11	0.91	0.90	0.94	0.62
KGE	0.98	0.44	0.96	0.96	0.97	0.79
KGElf	−1.14	0.02	−23.35	0.47	0.39	0.28
KGEnp	0.96	0.45	0.95	0.94	0.97	0.82
VE	1.09	1.46	1.11	1.11	1.08	1.30

MSE is measured in sq cm.

Table 8. Detailed Residual analysis for water table depth for SC monthly, growing and dormant season without daily-flow variable part 2.

	WS78_growing	WS78_dormant	WS80_daily	WS80_monthly	WS80_growing	WS80_dormant
ME	−1.50	−0.18	1.24	7.74	1.30	1.22
MAE	4.89	3.26	6.95	31.29	8.88	4.48
MSE	63.30	50.56	223.28	1479.47	304.14	101.81
RMSE	7.96	7.11	14.94	38.46	17.44	10.09
ubRMSE	7.81	7.11	14.89	37.68	17.39	10.02
NRMSE %	31.70	32.70	28.10	90.50	31.60	24.50
PBIAS %	2.30	0.60	−1.60	−9.20	−1.40	−2.20
RSR	0.32	0.33	0.28	0.91	0.32	0.24
rSD	1.04	0.99	1.01	1.00	1.03	1.01
NSE	0.90	0.89	0.92	0.16	0.90	0.94
mNSE	0.77	0.81	0.84	0.03	0.81	0.87
rNSE	0.90	0.44	−2.46	−0.76	0.63	0.25
wNSE	0.89	0.94	0.92	−0.10	0.90	0.93
d	0.98	0.97	0.98	0.76	0.98	0.99
dr	0.88	0.91	0.92	0.52	0.91	0.93
md	0.89	0.91	0.92	0.55	0.91	0.93
rd	0.98	0.86	0.14	0.51	0.91	0.81
cp	0.39	0.27	0.25	0.03	0.31	0.18
r	0.95	0.95	0.96	0.60	0.95	0.97
R2	0.90	0.89	0.92	0.16	0.90	0.94
bR2	0.88	0.88	0.90	0.14	0.89	0.92
KGE	0.93	0.95	0.96	0.59	0.94	0.96
KGElf	0.93	0.36	0.39	−0.06	0.38	0.53
KGEnp	0.94	0.96	0.95	0.52	0.94	0.96
VE	1.08	1.11	1.09	1.37	1.10	1.08

MSE is measured in sq cm.

7.4. Out of sample forecasts for WS80 for 2020

In various water table management systems, water table measurements are often discontinued for several days due to weather-related vulnerabilities and even discontinued in some cases due to budget constraints. However, obtaining biweekly forecast is crucial for preparing advanced precautionary management measures against flooding or sudden drop in water table in watersheds where time-periods are outside of the data collection window. In this study, we evaluated the performance of the 2020 model for WS80, which relies exclusively on daily meteorological data. The results of this analysis are presented in Table 9 for January, March, June, and October. This approach facilitates data assimilation, enabling stakeholders to incorporate newly available data to generate sub-seasonal forecasts. When hydroclimatic variables for future periods, such as biweekly intervals, become available, the pre-trained model can leverage these inputs to produce 14-day horizon predictions. This capability supports early warning for proactive land and water management. Decision making including for surface soil water conditions are important for operations of

Table 9. Bi-weekly predictions and errors for different periods for WS80.

Testing: Jan1–Jan14, Training period: < 2020-01-01

	Date	Depth	Predicted	Error
1	2020-01-01	−15.30	−18.45	3.15
2	2020-01-02	−16.40	−21.27	4.87
3	2020-01-03	−17.70	−21.24	3.54
4	2020-01-04	−16.80	−22.29	5.49
5	2020-01-05	−17.60	−20.86	3.26
6	2020-01-06	−19.20	−23.96	4.76
7	2020-01-07	−16.60	−26.83	10.23
8	2020-01-08	−12.60	−29.24	16.64
9	2020-01-09	−14.90	−31.46	16.56
10	2020-01-10	−16.80	−33.71	16.91
11	2020-01-11	−17.30	−34.98	17.68
12	2020-01-12	−14.00	−34.22	20.22
13	2020-01-13	−8.40	−33.62	25.22
14	2020-01-14	−5.60	−29.85	24.25

Testing: Mar1–Mar14, Training period: < 2020-03-01

	Date	Depth	Predicted	Error
1	2020-03-01	−6.00	−11.80	5.80
2	2020-03-02	−7.50	−17.27	9.77
3	2020-03-03	−5.60	−21.54	15.94
4	2020-03-04	−4.60	−21.28	16.68
5	2020-03-05	−0.20	−16.76	16.56
6	2020-03-06	−1.60	−1.57	−0.03
7	2020-03-07	−3.40	−6.93	3.53
8	2020-03-08	−4.60	−13.96	9.36
9	2020-03-09	−5.90	−19.62	13.72
10	2020-03-10	−7.40	−24.25	16.85
11	2020-03-11	−9.10	−26.87	17.77
12	2020-03-12	−10.90	−30.32	19.42
13	2020-03-13	−13.30	−34.63	21.33
14	2020-03-14	−16.10	−38.82	22.72

Testing: June1–June14, Training period: < 2020-06-01

	Date	Depth	Predicted	Error
1	2020-06-01	−19.60	−21.54	1.94
2	2020-06-02	−24.30	−29.96	5.66
3	2020-06-03	−30.90	−38.17	7.27
4	2020-06-04	−38.00	−44.99	6.99
5	2020-06-05	−44.80	−48.52	3.72
6	2020-06-06	−52.50	−54.38	1.88
7	2020-06-07	−59.10	−59.21	0.11
8	2020-06-08	−63.70	−61.79	−1.91
9	2020-06-09	−52.60	−64.25	11.65
10	2020-06-10	−33.30	−61.30	28.00
11	2020-06-11	−23.10	−63.22	40.12
12	2020-06-12	−16.70	−59.38	42.68
13	2020-06-13	−17.70	−52.96	35.26
14	2020-06-14	−19.80	−57.31	37.51

Testing: Oct1–Oct14, Training period: < 2020-10-01

	Date	Depth	Predicted	Error
1	2020-10-01	−11.70	−16.48	4.78
2	2020-10-02	−13.60	−22.66	9.06
3	2020-10-03	−16.00	−26.89	10.89
4	2020-10-04	−18.50	−28.82	10.32
5	2020-10-05	−21.50	−29.17	7.67
6	2020-10-06	−23.00	−32.91	9.91
7	2020-10-07	−23.90	−31.41	7.51
8	2020-10-08	−28.20	−36.53	8.33
9	2020-10-09	−32.30	−41.09	8.79
10	2020-10-10	−35.20	−43.45	8.25
11	2020-10-11	−10.00	−41.61	31.61
12	2020-10-12	−10.40	−32.62	22.22
13	2020-10-13	−11.80	−34.37	22.57
14	2020-10-14	−13.30	−37.81	24.51

heavy machinery used during logging and dynamic hydroclimatic conditions. Different methods for interval estimation of coefficients can be found in Manna et al. (2024).

8. Discussions and conclusions

The vector autoregression (VAR) and vector autoregression with several covariates (VARX) have served as essential tools in forecasting multivariate time series. In the presence of a high number of covariates, it becomes critical to choose the important covariates. We found that some packages handle multivariate data with sparsity assumptions such as "glmnet", but do not incorporate a time-dependent framework. Also, there is significant research on the autoregressive process with the presence of covariates (VARX), but incorporating variables with their lag is not too much explored. In our scenario, this factor is crucial for example, rainfall of the current day might not immediately affect the current water table depth.

Moreover, the water table depth of the previous couple of days might be one key variable that can be used to predict the current water table depth as they are highly correlated. On top of that, we want to do variable selection to understand which covariates and their lag are important for the explainability of water table depth. We could not find any parallel methodology that does handle suitably three major flexibilities: a) prediction under sparsity assumption within coefficients, b) considers a time series autoregression framework, and c) allows lags present in both dependent and independent variables, apart from "BigVAR" in the large interpretable family of linear models. We found the prediction for the daily level data is very good based on the computed model evaluation statistics. In different practical scenarios, the monthly average prediction is not recommendable based on monthly storage data as it does not capture the daily level variability. We also obtained a similar inference in the Table 2 where the adjusted R square is approximately poor with a minimum of .14 in comparison with the daily level and seasonal variation with a minimum adjusted square of .90. We recommend daily water table prediction, the growing and dormant seasonal level prediction through our model.

Groundwater models can be applied to research and management questions related to forest hydrology to focus on the movement and transport of subsurface flows through saturated porous media. Groundwater models typically are bounded by deep subsurface flow networks that reach across multiple catchment boundaries and use Darcy's flow equation (i.e., the groundwater flow equation) to estimate deep groundwater transport, which is based on relationships among hydraulic conductivity, hydraulic gradient, fluid flow rates, and the model domain contributing area (Golden et al. 2016). MODFLOW developed by USGS (Harbaugh 2005) is a process-based groundwater model that simulates three-dimensional saturated groundwater flow and storage, one-dimensional unsaturated flow, and groundwater interaction with streams. The mathematical method in MODFLOW is finite difference in space and time, with backward difference for time. MODFLOW assumptions are the following: (1) confined three-dimensional flow with water-table approximations, and (2) principal directions of hydraulic conductivity are aligned with the coordinate axes. This model was developed primarily for simulating groundwater flow dynamics (ground water head and flow directions in the aquifer) in rather deeper aquifer systems of larger areas where the surface water interaction, particularly vertical flux of evapotranspiration loss is minimal. In addition, MODFLOW requires multiple data on hydraulic heads, hydrogeologic aquifer properties, and boundary conditions whereas DRAINMOD simulates water table depth at middle of two parallel drainage ditches which are generally 50-100 m apart in a forest or an agricultural land.

In testing alternative models, Hill (1998) states that better models will have "three attributes: better fit, weighted residuals that are more randomly distributed, and more realistic optimal parameter values" Similar site-specific empirical hydrologic models for five forested wetlands with different characteristics by analyzing long-term observed meteorological and hydrological data in Zhu et al. (2017). These wetlands represent typical cypress ponds/swamps, Carolina bays, pine flatwoods, drained pocosins, and natural bottomland hardwood ecosystems. This empirical model by Zhu et al. (2017), the proposed model, and DRAINMOD are designed to simulate water table just on unconfined shallow aquifers primarily on sediment sand soil layers which has minimal interaction with deeper confined aquifers below a restrictive clayey layer between the shallow and deep aquifers in sedimentary rocks, e.t.c and characterized more by geology than the soils. MODFLOW is versatile in the scenarios where it can be applied to simulate water table for both on confined and unconfined aquifers.

In the literature, for example, Amatya and Skaggs (2001) explored the water table in a shallow unconfined aquifer with the model DRAINMOD in a drained pine plantation of poorly drained soil. The model was based on drainage ditches, simulates interception, and evapotranspiration (ET) as the sum of canopy transpiration and soil evaporation, drainage, and surface runoff with the data from 1988 to 1997. As water table is a highly correlated variable with water table depth, we compared it with the results from Amatya and Skaggs (2001) assuming similar performance in our prediction interval. R^2 varies from .65 to .91. In comparison to that, performance of our model was consistently higher $R^2 > 90\%$ for daily, growing, and dormant seasons after considering a time series model. In Latimer et al. (2022, 177), it was found that another well discussed model, MIKE SHE only obtained NSE as .45 for daily water table depth prediction whereas using a statistical model "BigVAR", we obtained more than 90% NSE for daily, growing and dormant season. So in comparison to the available methods, such as MIKE SHE and DRAINMOD, auto regressive process based prediction is stable consistently and performing better over a large time interval in the recent testing period across four different spatial locations for daily, growing and dormant season. In "BigVAR" we found that previous couple of days' available water table depth can be used to predict future water table depth significantly through auto regressive process. So it depends only fewer external parameters and not limited to upland or lowland predictions described in Amatya et al. (2024). The proposed model is more empirical than process-based MIKESHE and DRAINMOD models which can be reasonably applied without calibration and validation but with they cannot do future predictions.

In the time series plots, for example, for WS80 in the years around 2004 and 2006 (Fig. 9), for WS78 in the year 2018, and for WS77 in the year 2017 (Fig. 8), we may observe that in few places Δ and $\times$ are away from each other. The reason is that when there is too much rainfall, the water table rises up, sometimes above the ground level 0 (>0). As more water is added to the saturation zone, the water table moves closer to the ground surface. When the water table depth is close or above the surface (>0), the water table's surface water flooding situation behaves differently. So we do concentrate in the water table data where the water table depth is below the surface (<0). Similar observations and explorations were already concluded in Amatya, Gregory, and Skaggs (2000) and Amatya et al. (2024) based on different types of soils and extreme weather conditions. In the daily level time series plots we can observe that the confidence interval in D1 (NC) is thicker than the daily time series prediction in WS77, WS78, and WS80. It helps us to interpret that there is more variability in D1 (NC), an energy-limited site, than in the soil moisture limited three stations in SC. We may also observe the heteroscedasticity in D1 compared to watersheds in SC in Fig. 12. Similar observations were also found in figure 8 of Amatya et al. (2020) that daily water table depth does significantly vary across both the moisture limited WS80 in SC and energy limited D1 in NC form 2003 to 2008.

To benchmark the predictive performance of BigVAR, we compare its daily water table forecasts against a Bayesian autoregressive model previously applied to well WS77 (Table 4 in Manna and Ghosh 2025). While the Bayesian model achieves reasonable accuracy across multiple forecast horizons, BigVAR demonstrates comparable performance across multiple wells, with regression slopes near unity, Nash-Sutcliffe efficiencies exceeding 0.90, and root mean squared errors (Table 1). The average RMSE is 18.3 cm in the Bayesian Machine learning method, whereas BigVAR is 8.7–15.5 cm in daily prediction. Importantly, BigVAR leverages the multivariate and autoregressive structure of hydroclimatic and neighboring well data in the frequentist domain. These results highlight the strength of BigVAR for operational water-table forecasting, offering high predictive accuracy and the ability to handle multiple correlated time series simultaneously, making it a particularly suitable tool for wetland and watershed management applications.

The practical implication of the paper is that the proposed model can reliably forecast daily water-table depth using hydro-climatic inputs up to one week, enabling wetland and groundwater managers to make informed decisions and adapt to changing conditions. After one week, like other autoregressive models, the prediction error has increased.

The conclusions are drawn as follows:

- BigVAR is a tools for modeling sparse high-dimensional multivariate time series, which is moderately fast and efficient in computation. AR, VAR, and VARX are technical approaches that can help predict water table depth. BigVAR based model is another model like DRAINMOD which simulates 1-D (vertical) water table for a given point location of interest.
- Bigvar can be utilized as a predictive model for water table depth prediction with reasonably good performance and interpretability of the variable selection.
- Approximately 70% coefficients, we conclude they are sparse in daily prediction.
- Different climate variables can describe water table dynamics. The lag structure in the model plays a key role in estimating water table depth. Using the nearest previous water table depth estimates at any given time can create a suitable predictive model for water table dynamics. Additionally, we incorporate key weather variables along with their lagged effects.

  Variables such as rainfall, solar radiation, net radiation, and wind direction substantially improve the predictive performance of the model. These important variable selections are similar to Manna and Ghosh (2025) where solar radiation, net radiation, and wind directions are concluded as important covariates. solar radiation is a critical component in determining evapotranspiration (ET), which is a dominant factor affecting water table depth. High solar radiation promotes increased plant transpiration, which can lead to fluctuations in the water table. Studies have shown that forests exhibit higher daily evapotranspiration rates compared to other land covers, primarily because trees use water more effectively. For instance, forested areas can experience ET rates ranging from 5.02 to 6.32 mm/day, which is substantially greater than that of grassland or corn crops, demonstrating the direct impact of solar energy on plant water demand (Schilling (2007)).

  Additionally, solar radiation maintains plant function and phenology, correlating with groundwater recharge processes in healthy and dense forest landscapes. Wind direction and speed also play an important role in the water dynamics of forested watersheds by affecting evapotranspiration and influencing microclimates. Variations in wind can modulate evaporation rates and transpiration efficiencies of plants. Increased wind speed enhances evapotranspiration by removing moisture from leaf surfaces more rapidly, significantly impacting water table depths. Research indicates that groundwater levels often display diurnal patterns linked to both wind patterns and solar radiation, where interactions lead to distinct rises and falls of groundwater in response to daily plant water use (Butler Jr et al. 2007; Loheide, Butler Jr, and Gorelick 2005). Furthermore, localized wind patterns influenced by landscape features can create a microclimate that either favors or inhibits water table replenishment, underscoring the importance of wind direction in hydrological assessments.

If water table depth measurement is discontinued, it can still be predicted by solely different hydroclimatic variables if one has a pre-trained model as described in Sec. 7.4.

- Out-of-sample predictions tend to deviate increasingly from actual water depths over time, especially in later months like June in Table 9. This could indicate a challenge in maintaining model accuracy over longer durations. This might suggest seasonality or external factors influencing the predictions (e.g., environmental changes affecting depth measurements). The model performs better in predicting near-term values (e.g., Jan 1–Jan 7) and struggles with later-term predictions in each period, suggesting overfitting to initial data or underfitting to long-term patterns.

This study presents a modeling framework employing BigVAR with elastic net regularization to forecast daily water table depths. The approach effectively captures linear temporal dependencies while enabling automated variable selection, offering interpretability and computational efficiency. Our results demonstrate that even relatively simple autoregressive structures, when combined with regularization, can produce reasonable daily-scale predictions in hydrological contexts.

Nonetheless, several limitations should be noted. The inherent linearity assumption within BigVAR and related vector autoregressive models may inadequately represent the complex, nonlinear dynamics characteristic of groundwater systems. Hydrological processes—such as stormwater responses, evapotranspiration variability, and subsurface feedback—often involve nonlinear and threshold behaviors not fully captured by linear time series models. Future work could consider nonlinear methods, including machine learning approaches such as Random Forests or recurrent neural networks (e.g., LSTM) to better model these processes and potentially improve predictive accuracy (Breiman 2001; Hochreiter and Schmidhuber 1997).

The model assumes linear relationships between predictors and water table depth, which may limit its accuracy during extreme weather events. Nonlinear hydrological responses could lead to under- or over-prediction under such conditions. Although BigVAR employs regularization to control model complexity, high-dimensional predictor sets and long lag structures can still pose risks of overfitting, potentially reducing generalization. In our study, however, the number of hydroclimatic variables and selected lags is sufficiently modest that such overfitting concerns are unlikely to be substantial. These watersheds are small, homogeneous catchments, and stable climatic conditions prevail. Also, the hydrological behavior of the water table remains constant over a shorter time span, which supports our argument to apply autoregressive modeling, and assuming hydrological responses are linear holds good in this case.

Another important consideration is the stationarity assumption implicit in autoregressive frameworks. Although penalized regression techniques and differencing can partially mitigate non-stationarity, the evolving climatic and environmental conditions, alongside seasonal vegetation effects and anthropogenic impacts, limit the model's ability to generalize across extended periods or diverse hydrological regimes. Addressing non-stationarity explicitly through time-varying coefficient models or regime-switching frameworks may enhance model robustness (Hamilton 1989; Hastie and Tibshirani 1993).

We evaluated the temporal structure in model residuals using the autocorrelation function (ACF). For the first three locations, residual autocorrelations remained close to zero across lags, indicating minimal temporal dependence and suggesting that the autoregressive structure captures short-term dynamics effectively. In contrast, the fourth location exhibited substantial positive autocorrelation, with lag-1 correlation exceeding 0.5 and sustained dependence across subsequent lags, suggesting that additional lagged predictors or location-specific dynamics may be required to fully explain temporal variation. Overall, these diagnostics support the adequacy of the model for most sites while highlighting spatial heterogeneity in groundwater behavior.

Spatial dependence across monitoring wells was not incorporated in the present model due to the limited number of sites, which constrains the feasibility of spatial statistical methods. Nonetheless, groundwater levels are spatially correlated through underlying watershed characteristics such as soil texture, topography, and land cover. Incorporating spatial dependence via Gaussian process models or spatio-temporal hierarchical Bayesian models could yield more physically consistent and accurate forecasts (Banerjee, Carlin, and Gelfand 2014; Cressie 1993). The integration of spatial information represents a promising direction for future research.

Lastly, the model's predictive performance varied by temporal aggregation scale. In particular, the low coefficient of determination for monthly average predictions suggests that linear autoregressive models calibrated at daily resolutions may not be appropriate for coarser temporal scales. This finding highlights the trade-off between model interpretability and accuracy, motivating the exploration of models tailored to different temporal resolutions.

In conclusion, while the BigVAR-based elastic net approach provides a useful and interpretable baseline for daily water table forecasting, advancing groundwater predictive modeling will benefit from addressing nonlinear dynamics, nonstationarity, and spatial dependence. Ongoing work aims to incorporate these complexities and to evaluate hybrid modeling frameworks for improved hydrological inference and forecasting.

9. Recommendations and future goals

We do highly recommend to utilize a time series auto regressive model where we can incorporate water table depth lag values in addition to different climate variables with different lag structures for predicting water table depth. This model is well developed in theory and practice. In many scenarios, practitioners include different covariates based on their experience. “BigVAR” allows a penalized regression to do variable selection for inference and utilize that model for prediction. We want to explore the following directions in the future:

- Determine the instances duration and frequency within both the observed and simulated data where the water table depth remained within 30 cm for 14 consecutive days for wetland hydrology conditions.
- Explore the implementation of a hierarchical structure, for example Manna and Ghosh (2025) to manage missing data. In the current study, days with any missing variables were discarded. Investigate whether new data imputation methods could enhance our predictions. A better confidence interval for the estimates or water table depth should be also considered for time series data as mentioned in Manna et al. (2025a).
- A valuable future direction is to systematically investigate how seasonal patterns influence model performance by incorporating explicit seasonal decomposition or Fourier-based components, enabling a deeper understanding of seasonal effects on water table prediction.
- Consider developing a more complex spatiotemporal model using a larger dataset from various locations to improve prediction and interpretation. Is it feasible to create a model for a broader region, such as the entire state of South Carolina or the United States? Incorporating factors such as the distance and elevation of oceans, different watersheds, and the locations of wells may lead to better predictive models.
- Develop Models for predicting water table through spatial smoothing and uncertainties quantification which can predict where no monitoring data is available in 2-D or 3-D setup. For now, it was out of scope in our study as we require a larger database to encounter more variability across different locations.
- Through the use of priors, Bayesian models can naturally introduce regularization. For instance, priors like the spike-and-slab or horseshoe priors encourage sparsity, effectively shrinking less important parameters towards zero without manually tuning penalties as in ridge or Lasso regressions. A new model development in parallel to “BigVAR” is also under consideration for future research. Note that, In hydrological modeling, the primary goal

is often short- to medium-term forecasting rather than long-term seasonal analysis. While seasonality can be important for understanding annual patterns, our focus is on capturing daily and weekly dynamics that directly influence water table fluctuations. BigVAR efficiently models multivariate and autoregressive dependencies across wells without explicitly decomposing seasonal components, allowing accurate short-term predictions which is the main focus of the work. For studies requiring long-term seasonal trends, preprocessing or seasonal adjustments can be applied prior to model fitting.

- Long-term changes in climate, including shifts in precipitation patterns, temperature, and extreme weather events, may alter the underlying relationships captured by the model. As a result, the predictive capability of models trained on historical data could degrade over time. Practitioners should consider periodically retraining or updating the model with recent observations to maintain accuracy under evolving climatic conditions.
- If monitoring locations are available across multiple regions or climate zones, one can study spatio-temporal dynamics using hierarchical Bayesian models to capture regional heterogeneity and temporal evolution, as in Manna, Spencer, and Dey (2026).

Remark 2. The sparsity-aware autoregressive framework developed in this work provides a general methodology for forecasting high-dimensional temporal systems where (i) many lagged predictors are available and (ii) only a small subset meaningfully contributes to predictive skill. While our empirical focus is long-term groundwater forecasting across hydroclimatic drivers, the methodological components; particularly lag-based dependence modeling, Granger-style interpretability via sparse coefficients, and scalable estimation in a high-dimensional regime; naturally extend to several cross-disciplinary application domains. Based on the reviewer's suggestions, we discuss the applicability of our model in different scenarios such as biomedical applications, environmental studies, engineering, e.t.c. in Remark 3–5.

Remark 3. Recent biomedical research increasingly uses machine learning to support clinical decision-making, but most studies rely on static feature sets or black-box models without explicit representation of lagged dependencies or principled variable selection. For example, multi-criteria decision frameworks for optimal drug selection (Ghorbani et al. 2025a, 2025b) and strategic medical resource allocation (Rezaei et al. 2025) use analytic hierarchy and multi-criteria reasoning, yet do not model longitudinal physiological responses or dynamic treatment effects. Similarly, studies in rheumatology and implant technology (Ye et al. 2025; Zhang et al. 2025) advance AI-guided clinical tools but rely primarily on static predictors, while clinical meta-analyses and systematic reviews (Ding et al. 2024) lack temporal forecasting components. Research on psychological resilience and therapeutic response prediction (Ghorbani et al. 2023) incorporates predictive modeling but does not impose sparsity on temporal dependencies.

In these contexts, our autoregressive variable selection approach can (i) identify minimal biomarker sets that predict treatment outcomes through time, (ii) quantify temporal lag structure between dosage, physiological response, and adverse events, and (iii) retain interpretability required in clinical decision-making. Future work should integrate high-frequency patient monitoring data with sparse dynamic modeling pipelines to produce clinically actionable time-dependent risk predictions.

Remark 4. Our proposed method is not limited to hydrological applications. Environmental studies increasingly leverage machine learning for climate-driven hydrologic forecasting (Lu et al. 2025), yet many such models are nonlinear neural approaches that lack transparency regarding which hydroclimatic drivers matter most and over what lag windows. Work on citizen-driven pollution surveillance (Voskanyan, Ghorbani, and Azodinia 2024) provides valuable sensing data but does not incorporate autoregressive structured modeling, thus limiting short-term anomaly forecasting. Our framework directly addresses these gaps by enabling (i) sparse identification of dominant climatic drivers, (ii) spatio-temporal multivariate lag structures, and (iii) interpretable forecasting suitable for environmental governance. Future research should combine citizen-sensor datasets with sparse multivariate AR modeling to produce early-warning signals for pollution and lake eutrophication events.

Remark 5. Engineering and reservoir studies often apply machine learning for prediction, but most rely on nonlinear deep learning without structured temporal dependence or coefficient-level interpretability. For example, machine learning studies on reservoir recovery, drilling dynamics, and oil rate estimation (Beheshtian et al. 2024b, 2024a; Hazbeh et al. 2022) demonstrate predictive advances but without explicit sparse lag modeling. Work on geomechanical failure and sand production (Ghorbani and Abad 2022) and polymer injection processes (Tehrani et al. 2022) applies physics-based reasoning but lacks data-driven autoregressive modeling. Studies predicting reservoir quality (Hu et al. 2025) and petrophysical dynamics (Deng et al. 2025) employ sequential deep learning yet do not prioritize variable selection or explainability.

Our methodology can serve as a hybrid bridge between physics-based constraints and interpretable data-driven predictions. Sparse autoregressive models can (i) identify minimal operational parameters that drive well performance across lags, (ii) integrate physical variables as constrained predictors, and (iii) provide interpretable alternatives to deep networks in high-stakes engineering decisions. Future research should explore constrained sparse-AR models that embed reservoir physics while producing operational forecasts with uncertainty quantification.

Beyond domain applications, several methodological extensions warrant further study:

- **Time-varying and seasonal coefficients** to capture regime-dependent hydrologic response.
- **Nonlinear residual components** layered atop sparse linear lags for hybrid interpretable–nonlinear models.
- **Causal discovery** using sparse VAR structures for testing driver-response relationships.
- **Uncertainty quantification** through conformal or Bayesian variants of penalized autoregressive models.

These extensions would generalize our modeling framework from predictive analytics toward mechanistic inference, enabling deployment in regulatory, engineering, and clinical decision support contexts.

Acknowledgments

This research was partly supported by an appointment with the National Science Foundation (NSF) Mathematical Sciences Graduate Internship (MSGI) Program. This program is administered by the Oak Ridge Institute for Science and Education (ORISE) through an interagency agreement between the U.S. Department of Energy (DOE) and NSF. ORISE is managed for DOE by ORAU. All opinions expressed in this paper are the author's and do not necessarily reflect the policies and views of NSF, ORAU/ORISE, Forest Service, or DOE. The authors also acknowledge Andy Harrison, Hydrology Technician, at US Forest Service Santee Experimental Forest for providing related data for South Carolina sites. Similarly, thanks are due to the Forest Service Forest Watershed Research unit for providing on-site support to visit the monitoring sites at the Santee Experimental Forest watersheds. Alokesh Manna would also like to thank his advisor Dr. Dipak Dey, a Board of Trustees Distinguished Professor in the Department of Statistics at the University of Connecticut for several necessary guidelines for this project and recommendations for the MSGI program. A preliminary version of our work is also available in Manna, Mehan, and Amatya (2024).

Author Credit statement

In this paper, Alokesh Manna (https://sites.google.com/view/alokesh-manna/home) served as the lead author, contributing to the writing, conceptualization, methodology, validation, formal analysis, and investigation. Sushant Mehan (https://www.sdstate.edu/directory/sushant-mehan) and Devendra M. Amatya (https://bae.ncsu.edu/people/dmamatya/) mentored Alokesh Manna by providing supervision, reviewing, providing literature support, and editing the manuscript valuable suggestions and critical comments. Devendra M. Amatya also provided the data source, which is publicly available and continuously monitored from his workstation at the Santee Experimental Forest, Center for Forest Watershed Research, Southern Research Station, U.S. Forest Service.

Supplementary material

In the supplementary material, we provide the details of the parameters that we used for Bigvar. We also keep the guidelines for the practical implementation of this model and additional considerations in the Remark 1. We include the residual plot in the supplementary material. A correlation plot for different variables for WS77, WS78, and WS80 is provided in the supplementary material.

Disclosure statement

On behalf of all authors, the corresponding author states that there is no conflict of interest.

Funding

No external research funding was received for this work. This project was completed as part of the NSF Mathematical Sciences Graduate Internship (MSGI) program (https://www.nsf.gov/events/nsf-mathematical-sciences-graduate-internship-msgi).

ORCID

Alokesh Manna http://orcid.org/0009-0007-7958-5273
Sushant Mehan http://orcid.org/0000-0002-1565-9591
Devendra M. Amatya http://orcid.org/0000-0003-2641-9267

References

Ahmed, Ali Najah, Ayman Yafouz, Ahmed H. Birima, Ozgur Kisi, Yuk Feng Huang, Mohsen Sherif, Ahmed Sefelnasr, and Ahmed El-Shafie. 2022. "Water Level Prediction Using Various Machine Learning Algorithms: A Case Study of Durian Tunggal River, Malaysia." *Engineering Applications of Computational Fluid Mechanics* 16 (1): 422–440.

Amatya, Devendra M, Timothy J. Callahan, Sourav Mukherjee, Charles A. Harrison, Carl C. Trettin, Andrzej Wałęga, Dariusz Młyński, and Kristen D. Emmett. 2024. "Hydrometeorological Trends in a Low-Gradient Forested Watershed on the Southeastern Atlantic Coastal Plain in the USA." *Hydrology* 11 (3): 31.

Amatya, Devendra M., Marcin Fialkowski, and Agnieszka Bitner. 2019. "A Daily Water Table Depth Computing Model for Poorly Drained Soils." *Wetlands* 39: 39–54.

Amatya, Devendra M., James D. Gregory, and R. W. Skaggs. 2000. "Effects of Controlled Drainage on Storm Event Hydrology in a Loblolly Pine Plantation" *JAWRA Journal of the American Water Resources Association* 36 (1): 175–190.

Amatya, Devendra M., Carl C. Trettin, Charles A. Harrison, and Julie A. Arnold. 2022. "Long-Term Hydro-Meteorology and Water Quality Data from Low-Gradient Catchments of Varying Scales on the Santee Experimental Forest, South Carolina." *Hydrological Processes* 36 (5): e14549.

Amatya, Devendra Man, and Richard Wayne Skaggs. 2001. "Hydrologic Modeling of a Drained Pine Plantation on Poorly Drained Soils." *Forest science* 47 (1): 103–114.

Amatya, D. M., G. M. Chescheir, T. M. Williams, R. W. Skaggs, and S. Tian. 2020. "Long-Term Water Table Dynamics of Forested Wetlands: Drivers and their Effects on Wetland Hydrology in the Southeastern Atlantic Coastal Plain." *Wetlands* 40 (1): 65–79.

Amatya, D. M., and R. W. Skaggs. 2011. "Long-Term Hydrology and Water Quality of a Drained Pine Plantation in North Carolina." *Transactions of the ASABE* 54 (6): 2087–2098.

Amoah, Joseph K. O., Devendra M. Amatya, and Soronnadi Nnaji. 2013. "Quantifying Watershed Surface Depression Storage: Determination and Application in a Hydrologic Model." *Hydrological Processes* 27 (17): 2401–2413.

Appelboom, T. W., G. M. Chescheir, R. W. Skaggs, J. W. Gilliam, and D. Amatya. 2006. "Temperature Coefficient for Modeling Denitrification in Surface Water Sediments Using the Mass

Transfer Coefficient." In *Hydrology and Management of Forested Wetlands, Proceedings of the International Conference, April 8-12, 2006, New Bern, North Carolina*, 25. American Society of Agricultural and Biological Engineers.

Baird, Andy J., and Rob G. Low. 2022. "The Water Table: Its Conceptual Basis, its Measurement and its Usefulness as a Hydrological Variable." *Hydrological Processes* 36 (6): e14622.

Banerjee, Sudipto, Bradley P. Carlin, and Alan E. Gelfand. 2014. *Hierarchical Modeling and Analysis for Spatial Data*. Boca Raton, FL: CRC Press.

Beheshtian, Saeed, Sara Kishan Roodbari, Hamzeh Ghorbani, Mohamadreza Azodinia, Mohamed Mudabbir, and Annamaria R. Varkonyi-Koczy. 2024a. "Advanced Machine Learning Methods for Accurate Prediction of Loss Circulation in Drilling Well Log." In *2024 IEEE 11th International Conference on Computational Cybernetics and Cyber-Medical Systems (ICCC)*, 000031–000036. IEEE.

Beheshtian, Saeed, Sara Kishan Roodbari, Hamzeh Ghorbani, Mohamadreza Azodinia, Mohamed Mudabbir, and Annamaria R. Varkonyi-Koczy. 2024b. "Comparative Evaluation of Machine Learning and Bayesian Deep Learning Methods for Estimating Ultimate Recovery in Shale Well Reservoirs." In *2024 IEEE 11th International Conference on Computational Cybernetics and Cyber-Medical Systems (ICCC)*, 000017–000024. IEEE.

Breiman, Leo. 2001. "Random Forests." *Machine Learning* 45 (1): 5–32.

Butler Jr, James J., Gerard J. Kluitenberg, Donald O. Whittemore, Steven P. Loheide, Wei Jin, Mark A. Billinger, and Xiaoyong Zhan. 2007. "A Field Investigation of Phreatophyte-Induced Fluctuations in the Water Table." *Water Resources Research* 43 (2).

Cressie, Noel A. 1993. *Statistics for Spatial Data*. New York: Wiley.

Cui, Yali, and Jingli Shao. 2005. "The Role of Ground Water in Arid/Semiarid Ecosystems, Northwest China." *Groundwater* 43 (4): 471–477.

Dai, Z, C Li, C Trettin, G Sun, D Amatya, and H Li. 2010. "Bi-Criteria Evaluation of the MIKE SHE Model for a Forested Watershed on the South Carolina Coastal Plain." *Hydrology and Earth System Sciences* 14 (6): 1033–1046.

Dawn, Trisha, Angshuman Roy, Alokesh Manna, and Anil K Ghosh. 2021. "Some Clustering-based Change-point Detection Methods Applicable to High Dimension, Low Sample Size Data." arXiv preprint arXiv:2111.14012.

Dawn, Trisha, Angshuman Roy, Alokesh Manna, and Anil K Ghosh. 2025. "Some Clustering-based Change-Point Detection Methods Applicable to High Dimension, Low Sample Size Data." *Journal of Statistical Planning and Inference* 234: 106212.

Del Campo, Antonio D., Tarcísio J. G. Fernandes, and Antonio J. Molina. 2014. "Hydrology-Oriented (Adaptive) Silviculture in a Semiarid Pine Plantation: How Much Can Be Modified the Water Cycle through Forest Management?" *European Journal of Forest Research* 133: 879–894.

Deng, Changsheng, Yongke Wang, Weiwei Mi, Xiaofei Xie, Xining Sun, and Hamzeh Ghorbani. 2025. "Deep Learning-Driven Analysis of Petrophysical Dynamics in Pay Zone Quality and Reservoir Characterization." *Natural Resources Research* 34: 1–20.

Ding, Haiyang, Chuanguang Wang, Hamzeh Ghorbani, Sufang Yang, Harutyun Stepanyan, Guodao Zhang, Nan Zhou, and Wu Wang. 2024. "The Impact of Magnesium on Shivering Incidence in Cardiac Surgery Patients: A Systematic Review." *Heliyon* 10 (11): e32127.

Ghorbani, Hamzeh, and ARB Abad. 2022. "Analysis of Geomechanical Processes of Sand Production for Productive Wells (Study of Asmari Reservoir in the Ahvaz Oil Field)." *Bulletin of High Technology* 1: 10–18.

Ghorbani, Hamzeh, Sepideh Asadi, Simin Ghorbani, Parvin Ghorbani, Harutyun Stepanyan, Nina Khlghatyan, Diana Aghabalyan, Samaneh Bahrami, and Rituraj Rituraj. 2023. "Investigating the Predictive Contribution of Attitude Towards Life and Belief System on Self-Resilience and Psychological Toughness of Cancer Patients about the Mediating Role of Emotion Regulation." In *2023 IEEE 21st World Symposium on Applied Machine Intelligence and Informatics (SAMI)*, 000139–000146. IEEE.

Ghorbani, Hamzeh, Areg Chalabyan, Arsen Minasyan, Parvin Ghorbani, David A Wood, Simin Ghorbani, Rozi Yeremyan, Arpine Manasyan, and Fathema Zehra. 2025a. "Application of

Analytical Hierarchy Process to the Selection Suitability of Biological Drug forms for Psoriasis Treatment." *Journal of Pharmaceutical Innovation* 20 (3): 94.

Ghorbani, Hamzeh, Hrachuhi Papyan, Arsen Minasyan, David A. Wood, Parvin Ghorbani, Simin Ghorbani, Eduard Avagyan, Steve Badakian, and Natali Minasian. 2025b. "A Robust Multi-Criteria Decision-Making Approach for Selecting Optimal Drugs in Epilepsy Treatment Using the Analytic Hierarchy Process." *Brain Disorders* 20, 100292.

Golden, Heather E., Heather A. Sander, Charles R. Lane, Chang Zhao, Katie Price, Ellen D'Amico, and Jay R. Christensen. 2016. "Relative Effects of Geographically Isolated Wetlands on Streamflow: A Watershed-Scale Analysis." *Ecohydrology* 9 (1): 21–38.

Grace III, Johnny M., R. W. Skaggs, and G. M. Chescheir. 2006. "Hydrologic and Water Quality Effects of Thinning Loblolly Pine." *Transactions of the ASABE* 49 (3): 645–654.

Graham, Douglas N., and Michael B. Butts. 2005. "Flexible, Integrated Watershed Modelling with MIKE SHE." *Watershed models* 849336090: 245–272.

Hamilton, James D. 1989. "A New Approach to the Economic Analysis of Nonstationary Time Series and the Business Cycle." *Econometrica: Journal of the Econometric Society* 57: 357–384.

Hamilton, James D., and Raul Susmel. 1994. "Autoregressive Conditional Heteroskedasticity and Changes in Regime." *Journal of Econometrics* 64 (1–2): 307–333.

Harbaugh, Arlen W. 2005. *MODFLOW-2005, the US Geological Survey modular Ground-Water Model: The Ground-Water Flow Process*. Vol. 6. Reston, VA: US Department of the Interior, US Geological Survey.

Hastie, Trevor, and Robert Tibshirani. 1993. *Varying-Coefficient Models*. Vol. 55. Wiley Online Library.

Hazbeh, Omid, Hamzeh Ghorbani, Omid Molaei, Milad Shayanmanesh, Sahar Lajmorak, Rituraj Rituraj, and Samaneh Bahrami. 2022. "Proposing a New Model for Estimation of Oil Rate Passing through Wellhead Chokes in an Iranian Heavy Oil Field." In *2022 IEEE 22nd International Symposium on Computational Intelligence and Informatics and 8th IEEE International Conference on Recent Achievements in Mechatronics, Automation, Computer Science and Robotics (CINTI-MACRo)*, 000037–000044. IEEE.

Herath, Madhawa, Tharaka Jayathilaka, Yukinobu Hoshino, and Upaka Rathnayake. 2023. "Deep Machine Learning-based Water Level Prediction Model for Colombo Flood Detention Area." *Applied Sciences* 13 (4): 2194.

Hill, M. C. 1998. "Methods and Guidelines for Effective Model Calibration; with Application to UCODE, a Computer Code for Universal Inverse Modeling, and MODFLOWP, a Computer Code for Inverse Modeling with MODFLOW." Technical Report. US Geological Survey: Branch of Information Services [distributor].

Hochreiter, Sepp, and Jürgen Schmidhuber. 1997. "Long Short-Term Memory." *Neural computation* 9 (8): 1735–1780.

Hu, Xiao, Jun Xie, Xiwei Li, Junzheng Han, Zhengquan Zhao, and Hamzeh Ghorbani. 2025. "Predicting Hydrocarbon Reservoir Quality in Deepwater Sedimentary Systems Using Sequential Deep Learning Techniques." *Geomechanics and Geophysics for Geo-Energy and Geo-Resources* 11 (1): 96.

Imada, S., N. Yamanaka, and S. Tamai. 2008. "Water Table Depth Effects Populus Alba Fine Root Growth and Whole Plant Biomass." *Functional Ecology* 22 (6): 1018–1026.

Janssen, Joseph, Ardalan Tootchi, and Ali A. Ameli. 2024. "A Critical Appraisal of Water Table Depth Estimation: Challenges and Opportunities within Machine Learning." In *AGU Fall Meeting Abstracts*, Vol. 2024, H51L–0848.

Koch, Julian, Helen Berger, Hans Jørgen Henriksen, and Torben O. Sonnenborg. 2019. "Modelling of the Shallow Water Table at High Spatial Resolution Using Random Forests." *Hydrology and Earth System Sciences* 23 (11): 4603–4619.

Latimer, James S., David D. Bosch, John Faustini, Charles R. Lane, and Carl C. Trettin. 2022. "Enhancing Landscapes for Sustainable Intensification and Watershed Resiliency–Proceedings of the Seventh Interagency Conference on Research in the Watersheds." *General Technical Report 264, Asheville, NC: US Department of Agriculture Forest Service, Southern Research Station.* 264: 1–217.

Liu, Ziqiang, Xiaofang Ji, Limin Ye, and Jiang Jiang. 2022. "Inherent Water-Use Efficiency of Different Forest Ecosystems and its Relations to Climatic Variables." *Forests* 13 (5): 775.

Loheide, Steven P., James J. Butler Jr, and Steven M. Gorelick. 2005. "Estimation of Groundwater Consumption by Phreatophytes Using Diurnal Water Table Fluctuations: A Saturated-Unsaturated Flow Assessment." *Water Resources Research* 41 (7).

Lu, Xinyong, Zimo Wang, Menghao Zhao, Songzhe Peng, Song Geng, and Hamzeh Ghorbani. 2025. "Data-Driven Insights into Climate Change Effects on Groundwater Levels Using MaLhine learning." *Water Resources Management* 39 (7): 3521–3536.

Manna, Alokesh, and Sujit K. Ghosh. 2025. "Bayesian Models for Joint Selection of Features and Auto-Regressive Lags: Theory and Applications in Environmental and Financial Forecasting." arxiv. https://arxiv.org/abs/2508.10055.

Manna, Alokesh, Zijian Huang, Dipak K. Dey, and Yuwen Gu. 2024. "Interval Estimation of Coefficients in Penalized Regression Models of Insurance Data." arXiv preprint arXiv:2410.01008. https://arxiv.org/abs/2410.01008.

Manna, Alokesh, Sushant Mehan, and Devendra M. Amatya. 2024. "Development of a Statistical Predictive Model for Daily Water Table Depth and Important Variables Selection for Inference." arxiv. https://arxiv.org/abs/2410.01001.

Manna, Alokesh, Aditya Vikram Sett, Dipak K. Dey, Yuwen Gu, Elizabeth D. Schifano, and Jichao He. 2025a. "Distribution-Free Inference for LightGBM and GLM with Tweedie Loss." arXiv preprint arXiv:2507.06921 https://arxiv.org/abs/2507.06921.

Manna, Alokesh, Aditya Vikram Sett, Dipak K. Dey, Yuwen Gu, Elizabeth D. Schifano, and Jichao He. 2025b. "Supplemental Information: Conformal Prediction Inference in Regularized Insurance Models." *Applied Stochastic Models in Business and Industry* 41 (5): e70045.

Manna, Alokesh, Aditya Vikram Sett, Dipak K. Dey, Yuwen Gu, Elizabeth D. Schifano, and Jichao He. 2025c. "Conformal Prediction Inference in Regularized Insurance Models." *Applied Stochastic Models in Business and Industry* 41 (5): e70045.

Manna, Alokesh, Neil Spencer, and Dipak K. Dey. 2026. "Scalable Spatial Point Process Models for Forensic Footwear Analysis." arXiv https://arxiv.org/abs/2602.07006

Manrique-Alba, Angela, Antonio D. del Campo, and María Gonzalez-Sanchis. 2015. "Light Detection and Ranging for Implementing Water-Oriented Forest Management in a Semiarid Sub-Catchment (Valencia, Spain)." *CLEAN–Soil, Air, Water* 43 (11): 1488–1494.

Mehan, Sushant, Alokesh Manna, and Devendra Man Amatya. 2025. "Simulation of Water Table Depths in a Forested Wetland System in the Carolinas Using Data-Driven Approaches." *AGU25*.

Nguyen, Xuan Hoai and Thi-Thu-Hong Phan 2020. "Combining Statistical Machine Learning Models with ARIMA for Water Level Forecasting: The Case of the Red River." *Advances in Water Resources* 142: 103656.

Nicholson, W., D. Matteson, and J. Bien. 2019. "BigVAR: Dimension Reduction Methods for Multivariate Time Series." *R package version* 1 (4).

Nicholson, William, David Matteson, and Jacob Bien. 2017. "Bigvar: Tools for Modeling Sparse High-Dimensional Multivariate Time Series." arXiv preprint arXiv:1702.07094.

Pinno, Bradley D., Kazi L. Hossain, Ted Gooding, and Victor J. Lieffers. 2021. "Opportunities and Challenges for Intensive Silviculture in Alberta, Canada." *Forests* 12 (6): 791.

Rezaei, Jalal, Roya Azouji, Mina Azouji, and Hamzeh Ghorbani. 2025. "Application of the Analytical Hierarchy Process in the Management of Private Ambulance Care Systems in Three Selected European Countries: A Strategic Decision-Making Framework." *Frontiers in Public Health* 13: 1526586.

Salis, Matteo, Abdourrahmane M. Atto, Stefano Ferraris, and Rosa Meo. 2025. "Time Distributed Deep Learning Models for Purely Exogenous Forecasting: Application to Water Table Depth Predictions Using Weather Image Time Series." *Environmental Modelling & Software* 193: 106568.

Schilling, Keith E. 2007. "Water Table Fluctuations under Three Riparian Land Covers, Iowa (USA)." *Hydrological Processes: An International Journal* 21 (18): 2415–2424.

Ssegane, Herbert, Devendra M. Amatya, Augustine Muwamba, George M. Chescheir, Tim Appelboom, E. W. Tollner, J. E. Nettles, Mohamed A. Youssef, François Birgand, and R. W. Skaggs. 2017. "Calibration of Paired Watersheds: Utility of Moving Sums in Presence of Externalities." *Hydrological Processes* 31 (20): 3458–3471.

Sun, Ge, Hans Riekerk, and Nicholas B. Comerford. 1998. "Modeling the Forest Hydrology of Wetland-Upland Ecosystems in Florida 1." *JAWRA Journal of the American Water Resources Association* 34 (4): 827–841.

Tehrani, Pezhman Soltani, Hamzeh Ghorbani, Sahar Lajmorak, Omid Molaei, Ahmed Eid Ahmed Radwan, and Saeed Parvizi Ghaleh. 2022. "Laboratory Study of Polymer Injection into Heavy Oil Unconventional Reservoirs to Enhance Oil Recovery and Determination of Optimal Injection Concentration." *Geosciences* 8 (4): 579–592.

Tian, Shiying, Mohamed A. Youssef, R. Wayne Skaggs, Devendra M. Amatya, and G. M. Chescheir. 2012. "DRAINMOD-FOREST: Integrated Modeling of Hydrology, Soil Carbon and Nitrogen Dynamics, and Plant Growth for Drained Forests." *Journal of Environmental Quality* 41 (3): 764–782.

Vepraskas, M. J., R. W. Skaggs, and P. V. Caldwell. 2020. "Method to Assess Climate Change Impacts on Hydrologic Boundaries of Individual Wetlands." *Wetlands* 40: 365–376.

Voskanyan, Marine, Hamzeh Ghorbani, and Reza Azodinia. 2024. "Utilizing Citizen-Driven Scientific Endeavors for Freshwater Pollution Surveillance: A Case Report of Lake Sevan, Armenia." In *2024 IEEE 22nd World Symposium on Applied Machine Intelligence and Informatics (SAMI)*, 000505–000512. IEEE.

Wunsch, Andreas, Tanja Liesch, and Stefan Broda. 2020. "Groundwater Level Forecasting with Artificial Neural Networks: A Comparison of LSTM, CNN and NARX." *Hydrology and Earth System Sciences Discussions* 2020: 1–23.

Xuan, Yu, Anna Lamačová, Christopher Duffy, Pavel Krám, and Jakub Hruška. 2016. "Hydrological Model Uncertainty Due to Spatial Evapotranspiration Estimation Methods." *Computers & Geosciences* 90: 90–101.

Ye, Lusi, Xin Li, Hamzeh Ghorbani, Xiaofei Zhou, Arsen Minasyan, Bolun Zheng, Xiaotian Pan, Guodao Zhang, and Dan Chen. 2025. "Artificial Intelligence in Rheumatology: A Transformative Perspective." *Journal of Translational Internal Medicine* 13 (5): 390–393.

Zambrano-Bigiarini, Mauricio. 2017. "Package 'hydroGOF'." *Goodness-of-fit Functions for Comparison of Simulated and Observed*.

Zhang, Guodao, Rui Chen, Hamzeh Ghorbani, Wanqing Li, Arsen Minasyan, Yideng Huang, Sen Lin, and Minmin Shao. 2025. "Artificial Intelligence-Enabled Innovations in Cochlear Implant Technology: Advancing Auditory Prosthetics for Hearing Restoration." *Bioengineering & Translational Medicine* 10 (3): e10752.

Zhang, Xiaoying, Fan Dong, Guangquan Chen, and Zhenxue Dai. 2023. "Advance Prediction of Coastal Groundwater Levels with Temporal Convolutional and Long Short-Term Memory Networks." *Hydrology and Earth System Sciences* 27 (1): 83–96.

Zhang, Yangchengsi, Jiaqiang Du, Long Guo, Zhilu Sheng, Jinhua Wu, and Jing Zhang. 2021. "Water Conservation Estimation based on Time Series NDVI in the Yellow River Basin." *Remote Sensing* 13 (6): 1105.

Zhao, Tianxing, Yan Zhu, Ming Ye, Wei Mao, Xiaoping Zhang, Jinzhong Yang, and Jingwei Wu. 2020. "Machine-Learning Methods for Water Table Depth Prediction in Seasonal Freezing-Thawing Areas." *Groundwater* 58 (3): 419–431.

Zhu, Jie, Ge Sun, Wenhong Li, Yu Zhang, Guofang Miao, Asko Noormets, Steve G McNulty, John S King, Mukesh Kumar, and Xuan Wang. 2017. "Modeling the Potential Impacts of Climate Change on the Water Table Level of Selected Forested Wetlands in the Southeastern United States." *Hydrology and Earth System Sciences* 21 (12): 6289–6305.

Zhu, Senlin, Hongfang Lu, Mariusz Ptak, Jiangyu Dai, and Qingfeng Ji. 2020. "Lake Water-Level Fluctuation Forecasting Using Machine Learning Models: A Systematic Review." *Environmental Science and Pollution Research* 27: 44807–44819.